

# Groundwater-Surface water interactions: models to improve understanding of processes and dynamics in Baroota Creek, SA

Ву

**Phanumat Kullaboot** 

Thesis
Submitted to Flinders University
for the degree of

Master of Groundwater Hydrology

College of Science and Engineering
6th June 2025

# **Table of Contents**

1	INTRODUCTION	8
	1.1 Ephemeral and Intermittent Streams	8
	1.2 Groundwater Interaction- Surface water in Ephemeral Streams	9
	1.3 Study Aims	10
2	STUDY AREA	11
	2.1 Study Site	11
	2.2 Rainfall	13
	2.3 Surface Hydrology	16
	2.4 Geology and Hydrogeology	18
3	MATERIALS AND METHODS	24
	3.1 Fieldwork	24
	3.2 Streamflow Gauging	24
	3.3 Water arrival observation	28
	3.4 Light Detection and Ranging Survey (LiDAR)	31
	3.5 Conceptual Model of Ephemeral Baroota Creek	33
	3.6 Modelling Interface	33
	3.7 Model Setup	34
	3.8 Simulation Period and Initial Conditions	35
	3.9 Calibration and Simulation Scenarios	36
4	RESULTS	37
	4.1 Flow Gauging	37
	4.2 Creek Geometry and Cross-Sections	39
	4.3 Model Results	39
5	DISCUSSION	45
	5.1 Model Evaluation Against Field Observations	45
	5.2 Streamflow Scenarios and Groundwater Response	46
	5.3 Influence of Streambed Topography and Aquifer Simplification	47
	5.4 Limitations	48
	5.5 Future Directions	48
6	CONCLUSION	50
7	REFERENCES	51
8	APPENDICES	55
	8.1 Creek Geometry and Gauging measurement	
	8.2 Simulation period	

#### **Abstract**

Understanding streamflow generation in non-perennial rivers remains limited due to sparse data and the complexity of unsaturated and transient flow processes. This study contributes to address this gap by demonstrating how environmental flow released from the Baroota Reservoir influences groundwater and surface water (GW-SW) interactions in the Baroota Creek. Through a combination of field-based streamflow gauging and numerical modelling, the research characterised GW-SW interactions along a 3,450 m section of the creek. The study explored the efficiency of using a simplified surrogate model to accelerate simulation based on field hydrologic data collected at seven stream reaches. The results showed that there was high infiltration at the upstream reaches where coarse sediments, such as gravel and coarse sand, contribute to higher streambed hydraulic conductivity. In contrast, at the downstream reaches, which has finer sediments and lower creek bed elevation gradient, contributed to lower infiltration. The simplification of stream geometry and poorly constrained estimates of streambed hydraulic conductivity likely underestimate wetted perimeters and infiltration rates. Despite using a simplified conceptual model, the numerical model effectively captured spatial variability in surface water infiltration along the study reach. Overall, the study provides an initial step towards evaluating the success of managed flow releases intended to support riparian ecosystems. In particular, the benefits of environmental flows contributing to the River Red Gum woodland can reflect the biodiversity along these non-perennial river systems. Our findings have broader relevance for culturally inclusive water planning that aligns ecological restoration with First Nation values.

### Declaration

I certify that this thesis:

- 1. does not incorporate without acknowledgment any material previously submitted for a degree or diploma in any university
- 2. and the research within will not be submitted for any other future degree or diploma without the permission of Flinders University; and
- 3. to the best of my knowledge and belief, does not contain any material previously published or written by another person except where due reference is made in the text; and
- 4. does not use artificial intelligence (AI) to generate original ideas. AI was only used for grammar proofreading purposes.

Signed Phanumat Kullaboot				
Date	6th June 2025			

## Acknowledgements

I am deeply thankful for the scholarship provided by the Thai Government, which made my Master's studies possible. My appreciation also extends to the Department of Groundwater Resources, Thailand for providing me invaluable field experience and establishing a strong foundation that was crucial for the experimental aspects of this research. Their support broadened my understanding beyond theoretical concepts, integrating practical insights essential for this project.

This research has significantly contributed to my growth in both academic knowledge and practical understanding of real-world field and modelling work, particularly concerning groundwater and surface water (GW-SW) interactions.

My sincere thanks go to my principal supervisor, Associate Professor Eddie Banks, for offering the opportunity to engage in this exciting research and conduct practical field study through the project. His invaluable suggestions and feedback were instrumental to my work.

I am also profoundly grateful to my associate supervisor, Associate Professor Margaret Shanafield, for her valuable guidance and consistent support throughout the numerical modelling phase of this project. Her dedication to providing advice and assisting with initial model setup was greatly appreciated.

Special thanks are extended to Dr. Saskia Noorduijn for her encouragement and insightful advice on groundwater modelling, which was essential to this work. Her challenging questions often prompted deeper critical thinking regarding research gaps and experimental design.

I gratefully acknowledge our project collaborators, the Department for Environment and Water (DEW) South Australia and Landscape South Australia, for providing essential data and support.

I also appreciate the field assistance and valuable feedback received from colleagues at the National Centre for Groundwater Research and Training (NCGRT), Australia.

I am particularly thankful to Zoriana Lam, my study partner, whose collaborative insights and guidance on effective writing greatly enhanced both my academic communication and research methodology.

Finally, I would like to thank Thomas the cat, who loyally kept me company late into the night beside my computer, quietly monitoring my progress and providing emotional support throughout this research journey.

# **List of Figures**

Figure 1 An ephemeral stream in the dry (left) and with flow (right) in same location, the Baroota
Creek, South Australia.
Figure 2 The three main groundwater-surface water flow regimes. (A) A gaining stream occurs when
the aquifer drains into the stream. <b>(B)</b> In a losing-connected system, the stream loses water to the
aquifer; for both A and B, the connection between the stream and groundwater remains fully
saturated. <b>(C)</b> A losing-disconnected system, which is distinct due to the presence of an unsaturated
zone between the river and groundwater and results in infiltration rates becoming independent of
water table changes (based on Brunner et al., 2011 and Banerjee and Ganguly, 2023)
Figure 3 Study site in the semi-arid Baroota Creek Catchment where an environmental water release
event occurred from 22-30 <sup>th</sup> August 202412
Figure 4 Water released from the Baroota Reservoir flowing along Baroota Creek on August 24, 2024
(left), and River Red Gum trees (Eucalyptus camaldulensis) in the Baroota Creek area (right) 13
Figure 5 Rainfall gauging stations in the Baroota Creek area, SA by the Bureau of Meteorology (BOM).
Figure 6 Rainfall recorded from station 019120: Mambray Creek station with an average of 340 mm in
12 years from 2012 to 2024
Figure 7 Rainfall recorded from station 19037: Port Germein station with an average of 325 mm in 17
years from 2008 to 2024
Figure 8 Rainfall recorded from station 19112: Port Germein (Gowan Brae) station with an average of
365 mm in 17 years from 2008 to 2024
Figure 9 Map showing the entire length of the Baroota Creek discharging into Spencer Gulf at Port
Germein
Figure 10 The Baroota Creek morphology: upstream (left) - deep and narrow; downstream (right) -
wider and shallower
Figure 11 Geological map of the Baroota Creek area, South Australia
Figure 12 Hydrogeological map of the Baroota Creek area, South Australia
Figure 13 Groundwater observation wells in the Baroota Creek area
Figure 14 Groundwater levels recorded in well BTA 017 in the Baroota Creek area, with data up to
November 1989
Figure 15 Groundwater levels recorded in well BTA 028 in the Baroota Creek area, with data updated
until April 2025
Figure 16 Groundwater levels recorded in well BTA 028 in the Baroota Creek area, with data updated
until April 2025
Figure 17 Stream flow gauging sites in Baroota Creek, SA conducted between 24-25 August 2024 25
Figure 18 Streamflow Gauging measurement conducted in Baroota creek between 24 to 25 August
2024
Figure 19 Stream Discharge calculation total stream discharge developed based on USGS
Figure 20 Wetted perimeter parameters in trapezoidal channel geometry 28
Figure 21 Floodwave front tracking. Water arrival times were recorded at each point along Baroota
Creek following the environmental water released
Figure 22 Flood front observations in the Baroota Creek area during the environmental water released
in 22–25 August 2024
Figure 23 Map showing the locations of floodwave front tracking along Baroota Creek during the August
2024 environmental water release. Surface water was released from Baroota Reservoir at approximately
4:00 pm on 22 August 2024
Figure 24 LiDAR survey acquired along the study site section of the Baroota Creek using a DJI M300
drone in August 2024.
Figure 25 Concentual model of GW-SW interaction in Baroota creek area. South Australia

Figure 26 Baroota Creek streambed profile and delineation of stream segments	35
Figure 27 Conceptual Diagram for Floodwave Front Calibration in MODFLOW (Adapted fro	m Noorduijn
et al., 2014)	36
Figure 28 Calculated streamflow discharge (ML/day) during August 24-25, 2025	38
Figure 29 Comparison of Creek Geometry Derived from Gauging Measurements (Top) and	<b>GNSS</b> Data
(Bottom)	39
Figure 30 Simulated flow in the creek with initial discharge 114,048 m³/day (Scenario 1)	42
Figure 31 Simulated stream leakage with initial discharge 114,048 m³/day (Scenario 1)	42
Figure 32 Simulated flow in the creek with initial discharge 71,887 m³/day (Scenario 2)	43
Figure 33 Simulated groundwater head responding initial discharge 114,048 m³/day (Scenario	1)43
Figure 34 Simulated stream leakage with initial discharge 71,887 m <sup>3</sup> /day (Scenario 2)	44
Figure 35 Simulated groundwater head responding initial discharge 71,887 m³/day (Scenar	rio 2) 44

# **List of Tables**

Table 1. Identified stream segments along Baroota Creek	34
Table 2 Flow gauging measurement results at seven cross-sections in the Baroota creek area during	
24-25 August 2024	37
Table 3 Simulated streambed hydraulic conductivity (Ks) in model calibration in Scenario 1	41
<b>Table 4</b> Simulated streambed hydraulic conductivity (Ks) in model calibration in Scenario 2	41

#### 1 Introduction

In arid and semi-arid regions such as South Australia, groundwater is a vital resource for both human use and ecological sustainability. These regions are characterised by highly variable rainfall, low recharge rates, and intermittent streamflow, making groundwater–surface water (GW–SW) interactions especially important for maintaining environmental flows (e-flows) and supporting groundwater-dependent ecosystems (Zhong et al., 2023, Lamontagne et al., 2005). Aquifer recharging through non-perennial (ephemeral) streambeds has been identified as a key mechanism in sustaining groundwater levels in such settings (Shanafield and Cook, 2014, Quichimbo et al., 2020).

## 1.1 Ephemeral and Intermittent Streams

In arid and semi-arid regions watersheds often include ephemeral and intermittent streams as key hydrological features (Figure 1). Ephemeral stream, which lacks continuous flow, flow solely following rainfall events while the intermittent streams maintain flow in segments affected by groundwater discharge or temporal surface runoff (Levick et al., 2008). It is believed that groundwater recharge in these dry regions mainly relies on aquifer recharge through ephemeral streambeds (Shanafield and Cook, 2014, Quichimbo et al., 2020).

A key interface between groundwater and surface water is the hyporheic zone, which is a subsurface region where stream water mixes with shallow groundwater through porous bed and bank materials. This zone plays an important role in facilitating recharge, buffering stream temperature, and supporting biogeochemical processes vital for riparian ecosystems (Winter et al., 1998). In ephemeral dryland streams, infiltration into the hyporheic zone is especially critical for water exchange and ecological function (Wang et al., 2017).

In response to climate change and decreasing natural flows in these non-perennial rivers and streams, environmental flow releases have become an important water management strategy to restore ecological function in degraded riparian corridors. These managed flows aim to replicate components of the natural flow regime that support critical vegetation and ecosystem processes (Arthington et al., 2018). Understanding groundwater-surface water (GW-SW) interaction patterns in non-perennial is therefore essential for improving hydrological connectivity following environmental releases.





**Figure 1** An ephemeral stream in the dry (left) and with flow (right) in same location, the Baroota Creek, South Australia.

#### 1.2 Groundwater Interaction- Surface water in Ephemeral Streams

Historically, groundwater (GW) and surface water (SW) were considered separate components of the hydrological cycle and were often studied independently (Winter et al., 1998). However, they are now recognised as interconnected systems (Banerjee and Ganguly, 2023). In the mid-1950s, groundwater pumping was uncovered as global issues affecting stream flow, when groundwater and surface water interact to result as either gaining streams, with water received from the groundwater system, or losing streams, with water contributing to the underlying aquifer. (Banerjee and Ganguly, 2023, Brunner et al., 2011) (Figure 2). Therefore, studies in GW-SW interaction are common in evaluating river reaches at a local scale and as discrete systems, identifying streams as gaining, losing or losing disconnected streams (Winter et al., 1998, Cook et al., 2010, Brunner et al., 2011).

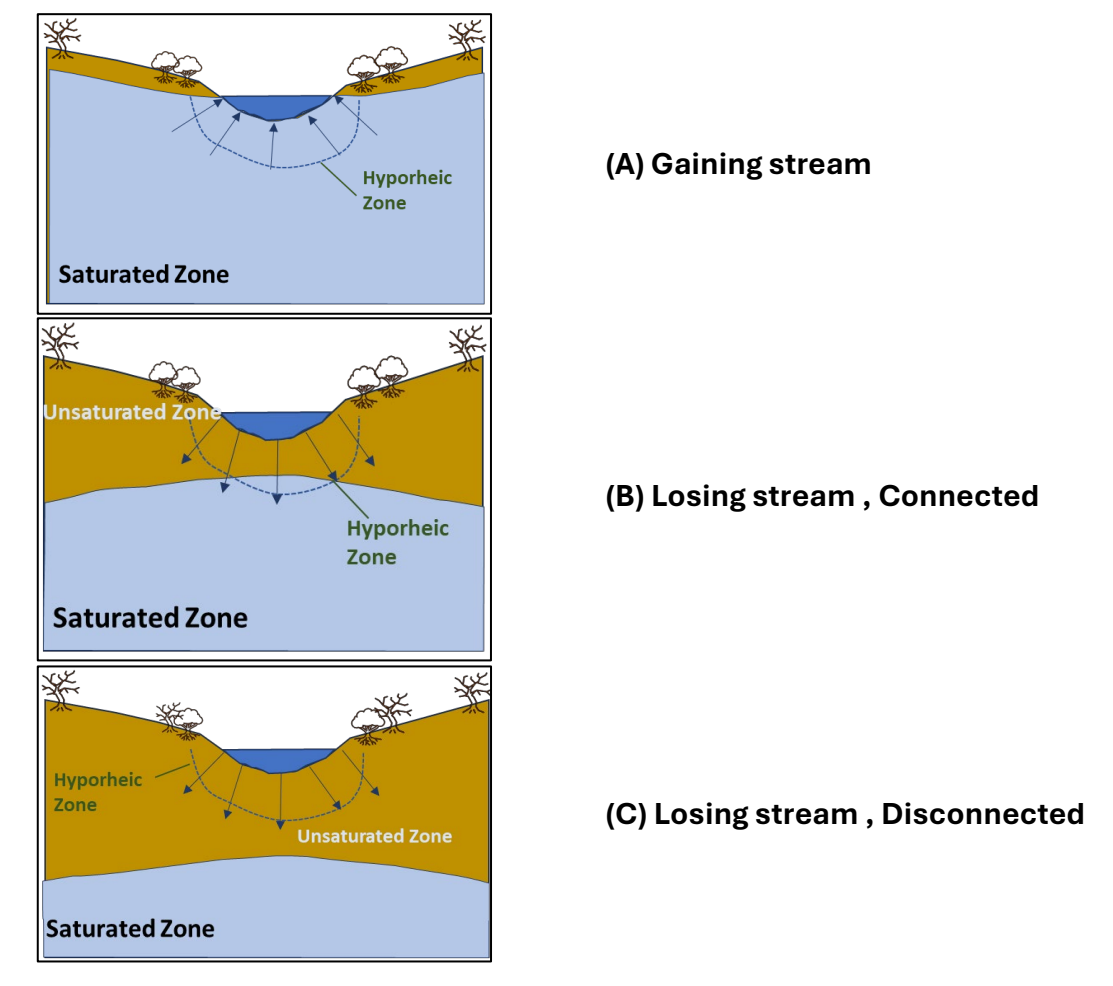


**Figure 2** The three main groundwater-surface water flow regimes. **(A)** A gaining stream occurs when the aquifer drains into the stream. **(B)** In a losing-connected system, the stream loses water to the aquifer; for both A and B, the connection between the stream and groundwater remains fully saturated. **(C)** A losing-disconnected system, which is distinct due to the presence of an unsaturated zone between the river and groundwater and results in infiltration rates becoming independent of water table changes (based on Brunner et al., 2011 and Banerjee and Ganguly, 2023).

### 1.3 Study Aims

This study aims to characterise interaction between groundwater and surface water within the riparian zone. The objective is to investigate the hydrological responses to these managed flow events, including their influence on GW-SW interactions and infiltration patterns in an arid catchment with deep watertables.

Specifically, in this study we:

- 1. Conducted an intensive streamflow gauging field survey at seven sites during an environmental flow release down Baroota Creek;
- 2. Developed a numerical model using the field survey and environmental flow data to quantify surface water infiltration losses;
- 3. Used the model to simulate variability in the recharge process along the stream reach.

By integrating hydrological monitoring, this research establishes a multidisciplinary framework for assessing the impact of environmental flows in order to understand the ecological role of groundwater in sustaining riparian ecosystems. We found that controlled flow releases can temporarily shift groundwater levels, enhancing surface groundwater connectivity. These findings can provide valuable insights on improving environmental water management and contribute to long-term planning of water resources to preserve the cultural heritage of the watershed in these semi-arid landscapes.

#### 2 Study Area

### 2.1 Study Site

The study site, Baroota Creek Catchment, is situated approximately 20 km northeast of Port Germein, located in the southern Flinders Ranges of South Australia (Figure 3). The available water resources in the region were allocated as part of the Baroota Prescribed Water Resources Area (BPWRA) on June 19, 2008 (DEW, November 2020) and declared under the Natural Resources Management Act 2004 since June 2008 (DEW, 2021, Evans, 2004b).

A key feature of the ephemeral Baroota Creek is the Baroota Reservoir. The reservoir was constructed in 1921 and is located at the top of the catchment, which is upstream of the Pirie Basin (Evans, 2004a). Initially built to control stream flow, the Baroota Reservoir now functions as an offline reservoir and no longer supplies drinking water (SA Water). The reservoir has prevented fewer natural flows down the ephemeral Baroota Creek and as a result environmental flows are periodically released from the Baroota Reservoir to sustain downstream ecosystems (Figure 4). The first environmental and cultural water release occurred in September 2022, aimed at enhancing River Red Gum resilience, recharging groundwater, and supporting the cultural responsibilities of the Nukunu people in caring for Country (The Landscape Boards South Australia, 2025a). This study focuses on a subsequent environmental flow release conducted in August 2024, which was designed to assess downstream infiltration patterns, ecological benefits, and groundwater-surface water interactions.

The riparian ecosystem along the lower reaches of the semi-arid Baroota Creek is dominated by River Red Gum (*Eucalyptus camaldulensis*), and is highly dependent on groundwater, especially from the shallow aquifer (Water, 2009-10). These trees are commonly found along rivers and creeks across Australia and serve as a key indicator of riparian health due to their reliance on accessible groundwater (SA Arid Lands Landscape Board, June 2010). Historically, overbank flows during winter and spring replenish groundwater and support the health of these ecosystems. However, dam and weir infrastructure have diminished these flows, leading to reduced recharge and increased stress on riparian vegetation.

Beyond its hydrological characteristics, the Baroota Creek area holds significant cultural importance as part of the traditional lands of the Nukunu people. This intrinsic link between ecological sustainability and cultural values underscores the importance of this research. A recent environmental and cultural water release from the Baroota Reservoir in 2022 (The Landscape Boards South Australia, 2025a), the first of its kind, aimed to enhance the health of local River Red Gum trees (*Eucalyptus camaldulensis*), which are high-value water dependent ecosystems in the PWRA. The release also facilitated groundwater recharge, and supported the Nukunu people in fulfilling their cultural obligations of caring for Country (The Landscape Boards South Australia, 2025b).

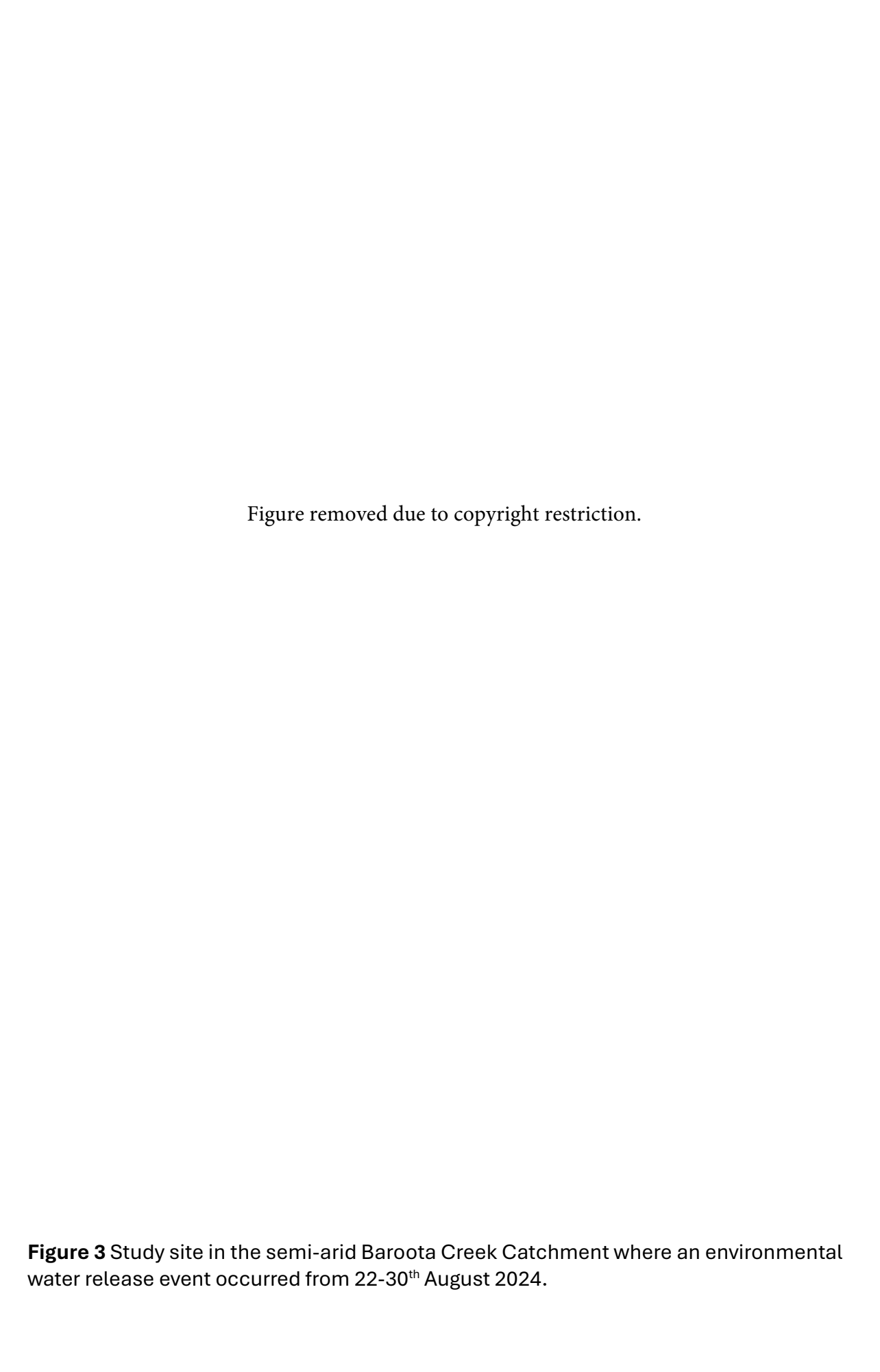


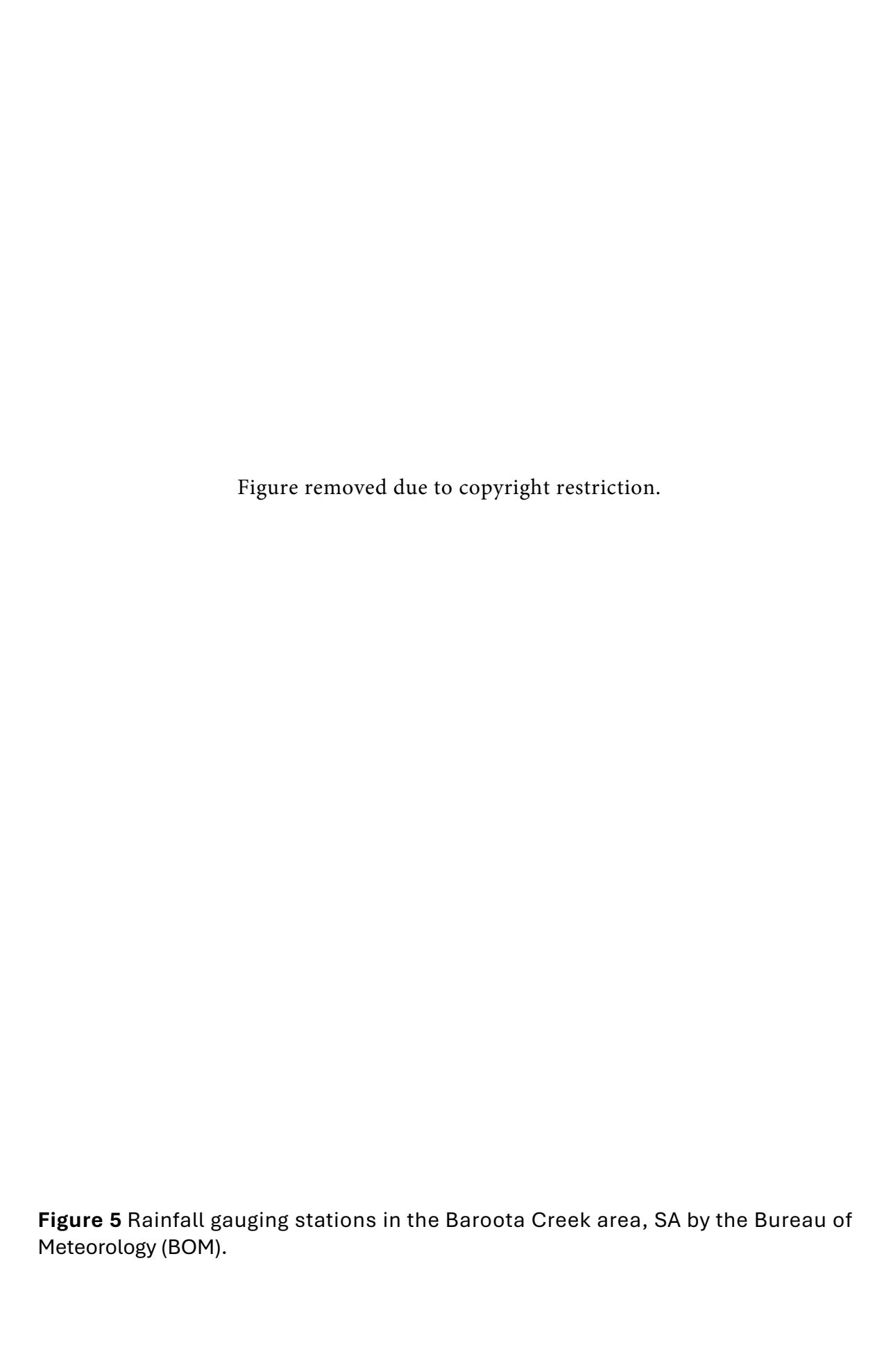




**Figure 4** Water released from the Baroota Reservoir flowing along Baroota Creek on August 24, 2024 (left), and River Red Gum trees (*Eucalyptus camaldulensis*) in the Baroota Creek area (right).

### 2.2 Rainfall

Rainfall data for the Baroota Creek area were obtained from three Bureau of Meteorology (BOM)stations (Figure 5). The first station 019120 at Mambray Creek, is situated approximately 8.4 km from the study area and recorded an average annual rainfall of 365 mm between 2008 and 2024 (Figure 6). The second station 019037 at Port Germein, is located about 11 km away, has a slightly lower average of 325.25 mm for the same period (Figure 7). The third station 19037 at Port Germein (Gowan Brae), approximately 14 km from the study area, has an average annual rainfall of 340 mm from 2012 to 2024 (Figure 8).



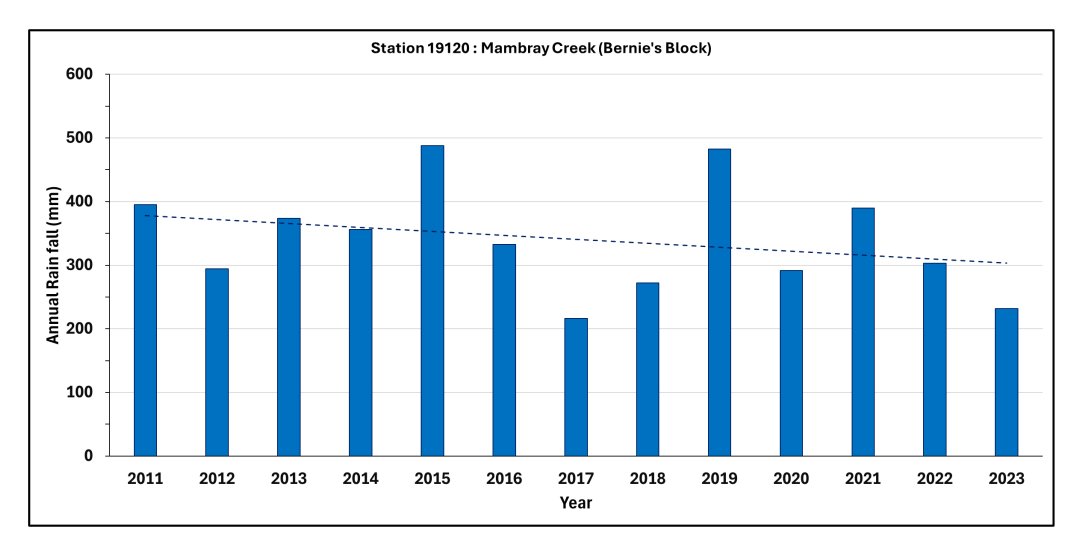


**Figure 6** Rainfall recorded from station 019120: Mambray Creek station with an average of 340 mm in 12 years from 2012 to 2024.

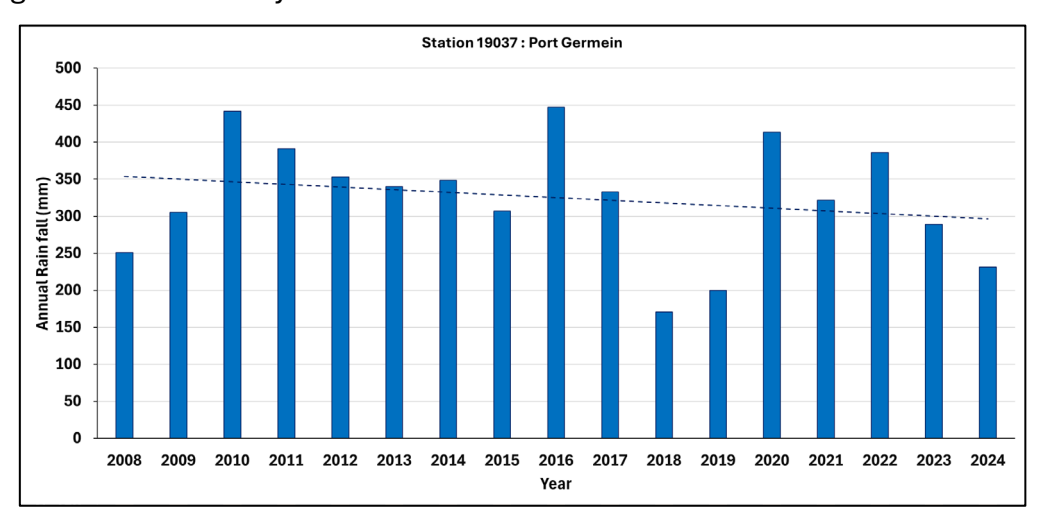


**Figure 7** Rainfall recorded from station 19037: Port Germein station with an average of 325 mm in 17 years from 2008 to 2024.

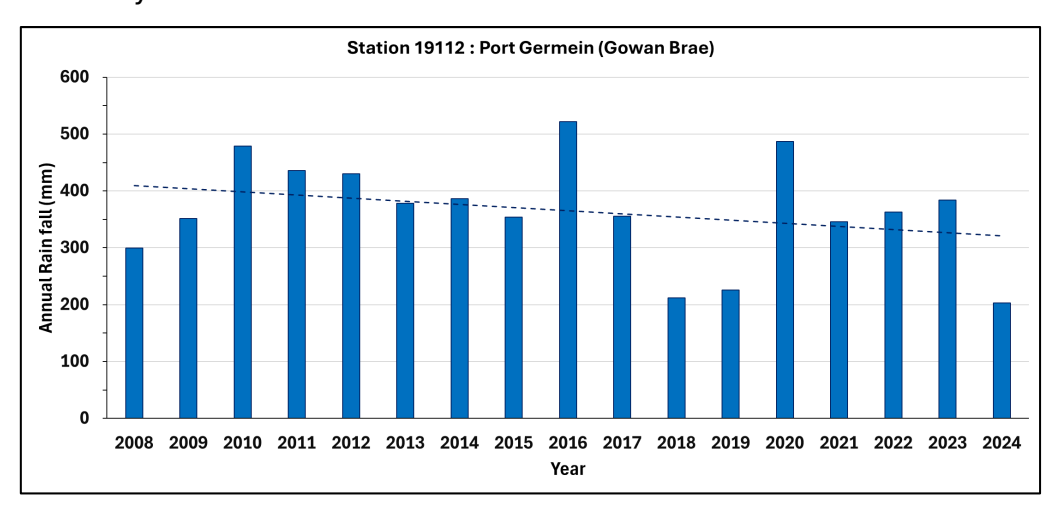


**Figure 8** Rainfall recorded from station 19112: Port Germein (Gowan Brae) station with an average of 365 mm in 17 years from 2008 to 2024.

# 2.3 Surface Hydrology

The Baroota Creek extends approximately 18,050 m downstream from the reservoir, flowing from northeast to southwest toward the Spencer Gulf at Port Germein (Figure 9). The creek's morphology varies along the water course. To illustrate, the upstream sections are typically narrow and incised, while the downstream reaches become broader and flatter, reflecting changes in channel gradient and sediment deposition (Figure 10).

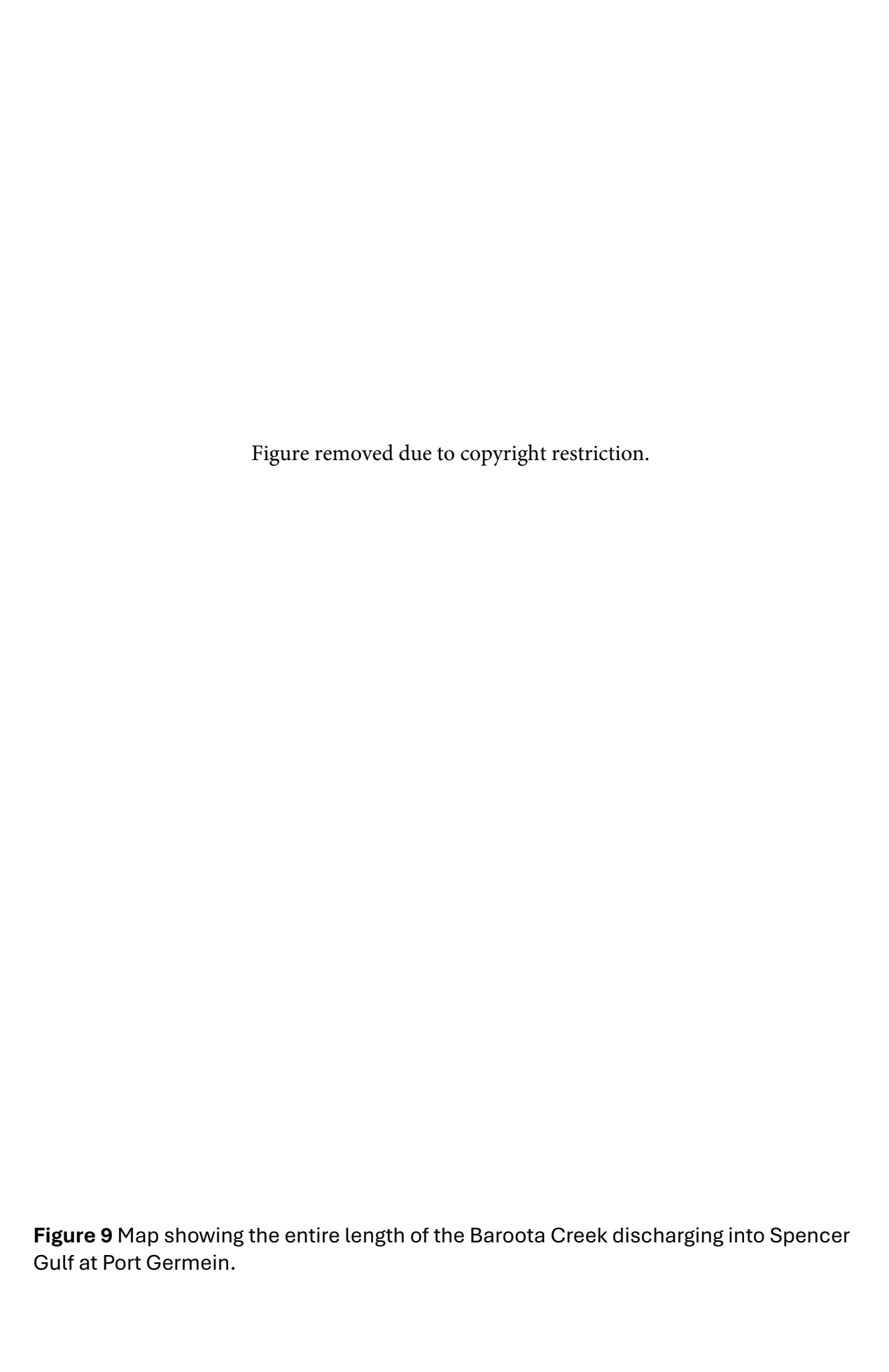






**Figure 10** The Baroota Creek morphology: upstream (left) - deep and narrow; downstream (right) - wider and shallower.

Baroota Creek is a highly modified ephemeral creek that only flows in response to high-intensity rainfall or controlled releases from Baroota Reservoir (DEWNR, 2014). A notable characteristic of the Baroota Reservoir is its continuous leakage, first observed shortly after its completion (Barnett, 2009). This leakage has been periodically quantified by measuring surface flow rates in the creek bed downstream of the reservoir since 1988, consistently providing an estimated 8 to 15 L/sec of recharge to the underlying aquifers. However, the precise volumes of subsurface flow through the creek bed's gravels and fractured rock remain unquantified (Evans, 2004a).

In addition to this consistent leakage, the dam experiences occasional overflow events. These overflows provide short, intense periods of recharge (lasting several days) through the highly permeable and gravelly bed of Baroota Creek (Evans, 2004a). For instance, during a 1989 overflow event, an estimated flow of 100 L/sec was recorded in Baroota Creek, approximately 500 m downstream of the reservoir. This flow significantly decreased to just 20 L/sec at further 3.5 km downstream (Clarke, 1990 in DEW, November, 2020).

#### 2.4 Geology and Hydrogeology

The Baroota Creek Catchment is located within the Pirie Basin, which the near-surface hydrostratigraphy considerable thickness of alluvial and fluvial Quaternary clays and gravels deposited as outwash from the Flinders Ranges (DEW, November 2020) (Figure 11). The streambed of the Baroota creek composed with highly permeable gravel beds within thickness extends to about 100 m (DEWNR, 2014, DEW, November 2020).

The creek primarily flows through channel and floodplain alluvium (Qa), consisting of gravel, sand, silt, and clay, which are locally calcreted and provide high permeability pathways for infiltration. Surrounding this are colluvial and residual deposits (Qrc), comprising boulders, gravels, and minor alluvium, which contribute to lateral groundwater movement across the plains. To the west, dune and sandplain units (Qd) with interdune claypans may locally restrict infiltration. Near the coast, Holocene

coastal sediments (Qe) form intertidal flats and marshes with low permeability, while the eastern highlands expose fractured bedrock (Ns) composed of tillite, sandstone, and dolomite (Figure 12). These fractured rock units near the reservoir are important for understanding potential leakage and subsurface flow. Overall, the geological variation along the creek influences hydrogeological processes, particularly infiltration dynamics and the potential for groundwater recharge during environmental flow events.

Groundwater observation well data in the Baroota Creek area were sourced from the South Australian Government's WaterConnect website (https://www.waterconnect.sa.gov.au) (Figure 13). However, this data has limitations, including being inconsistently updated across different monitoring locations. Based on more recent records from some wells, current groundwater levels are approximately 30 m below the surface. This study reports groundwater levels in metres relative to the Australian Height Datum (mAHD), where 0 m represents mean sea level.

To illustrate, BTA017 is a shallow upstream well (5.18 m deep), last water level recorded in 1989, showing an average groundwater level of 76.88 mAHD, approximately 3.2 m below the ground which has an elevation of 80.11 mAHD (Figure 14). In contrast, BTA028 is a deeper well (87 m deep), having stable water levels averaging 31.16 mAHD between 2015 and 2025, where the ground surface elevation is 75.06 mAHD, approximately 44 m below ground (Figure 15). In addition, BTA009 located downstream recorded from 2015 as 22.12 mAHD, approximately 32 m below its surface elevation of 54.11 mAHD (Figure 16).

Figure removed due to copyright restriction.

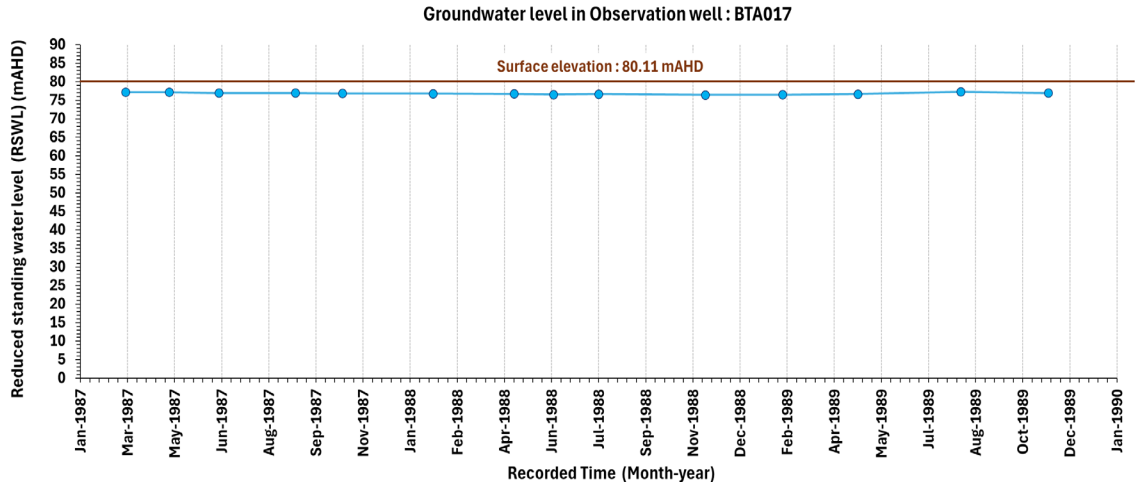
Figure 11 Geological map of the Baroota Creek area, South Australia.

Figure removed due to copyright restriction.

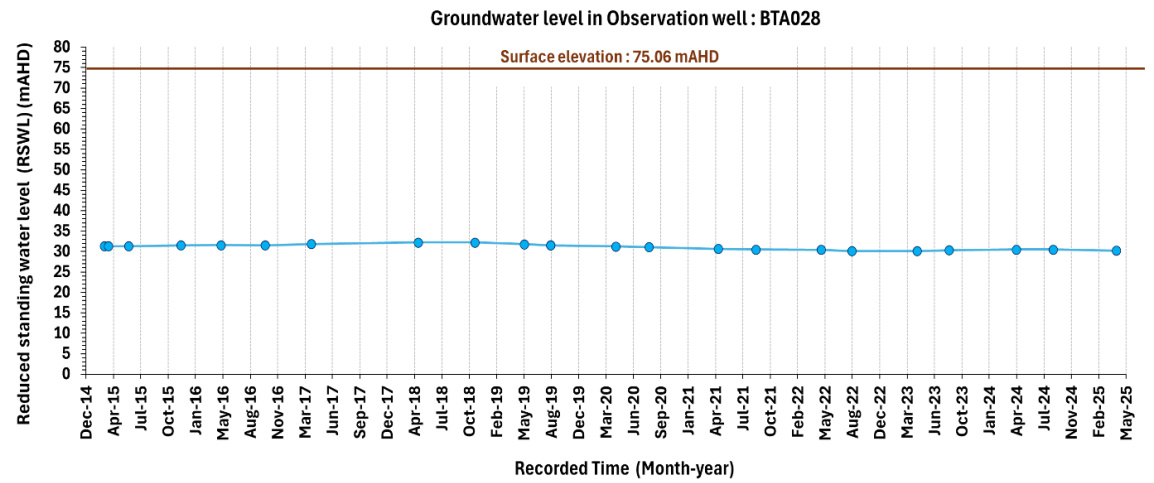
Figure 12 Hydrogeological map of the Baroota Creek area, South Australia.

Figure removed due to copyright restriction.

Figure 13 Groundwater observation wells in the Baroota Creek area.



**Figure 14** Groundwater levels recorded in well BTA 017 in the Baroota Creek area, with data up to November 1989.



**Figure 15** Groundwater levels recorded in well BTA 028 in the Baroota Creek area, with data updated until April 2025.

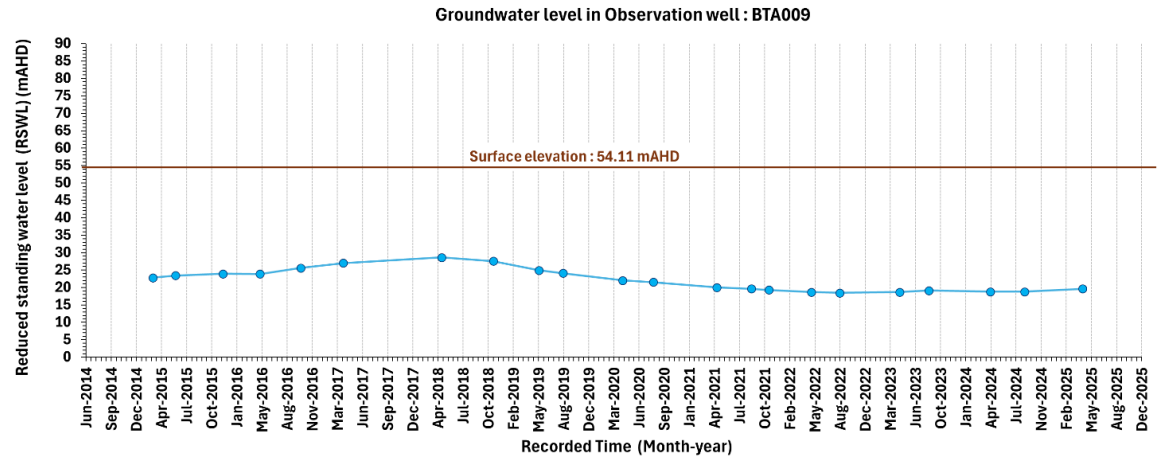


**Figure 16** Groundwater levels recorded in well BTA 028 in the Baroota Creek area, with data updated until April 2025.

#### 3 Materials and Methods

#### 3.1 Fieldwork

Fieldwork was conducted in the Baroota Creek area between 22 and 25 August 2024, coinciding with the managed environmental water release from Baroota Reservoir.

#### 3.2 Streamflow Gauging

Flow within the study reach was measured manually at seven cross-sections along Baroota Creek using the velocity-area method (Hipólito & Loureiro, 1988). Cross-section locations were selected based on accessibility and distribution to adequately represent the full length of the study area (Figure 17). Although the environmental water release from Baroota Reservoir began on 22 August 2024, the first available gauging was conducted on 24 August 2024. The gauging data was used to provide a boundary condition for the numerical model and to validate estimated downstream flows (Figure 18).

At each gauging site, the stream cross-section was subdivided into vertical segments spaced every 0.3 to 0.5 metres (m), depending on the creek's width and the required spatial resolution. For each segment, depth and velocity were measured using a Marsh McBirney Flo-Mate 2000, a portable electromagnetic flowmeter. The geographic coordinates of each cross-section were recorded using a Trimble GNSS receiver for accurate spatial referencing.

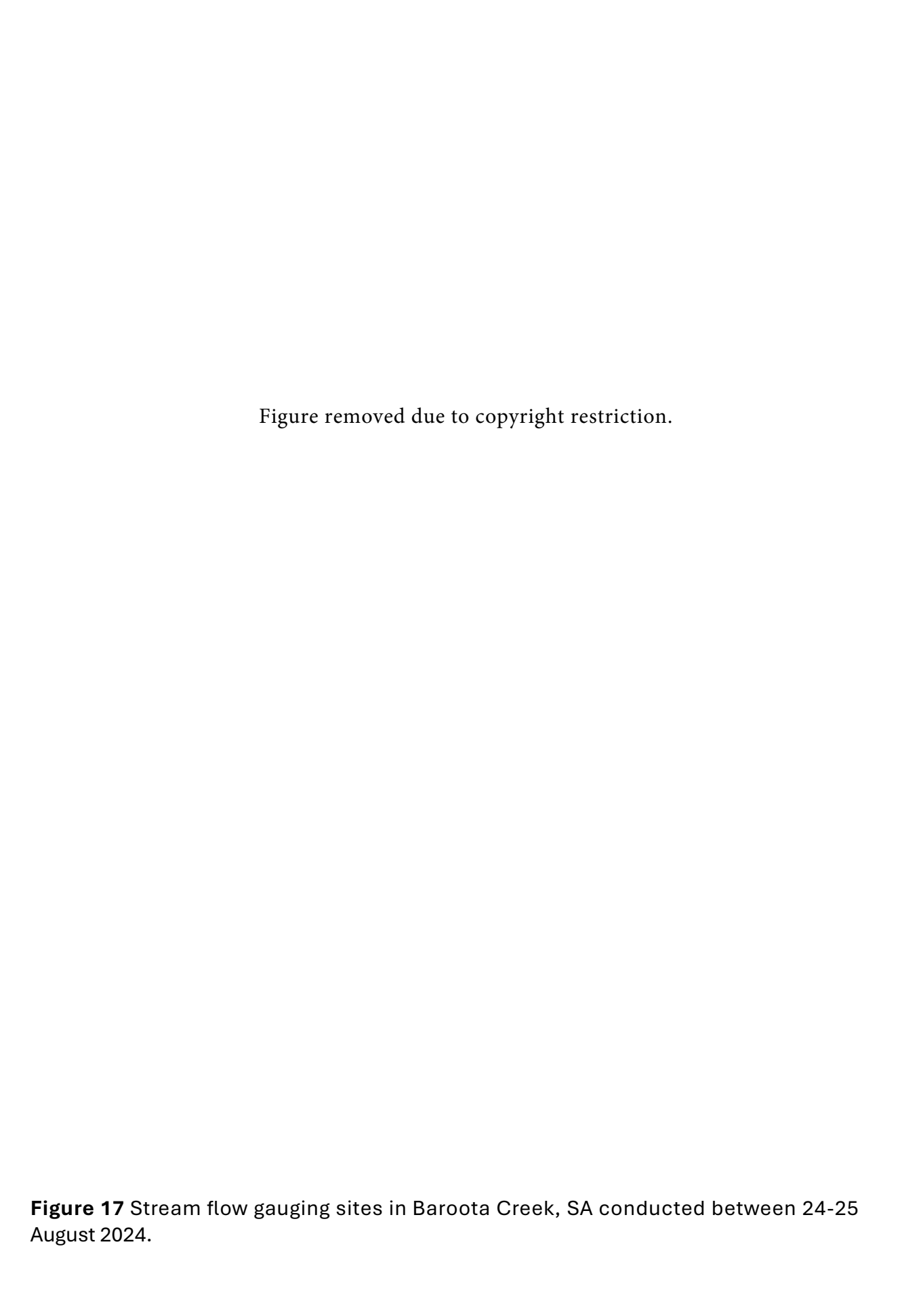






**Figure 18** Streamflow Gauging measurement conducted in Baroota creek between 24 to 25 August 2024

The velocity-area method is a widely accepted approach for calculating discharge (Q) in open-channel flow systems. The method involves calculating the flow in each vertical segment and summing all segment discharges to obtain the total stream discharge (Figure 19) (HipÓLito and Loureiro, 1988):

$$Q = \sum_{i=1}^{n} a_i v_i$$

Where Q is total discharge (m³/s)  $a_i$  is cross-section area (m²)  $v_i$  is the corresponding mean velocity (m/s)

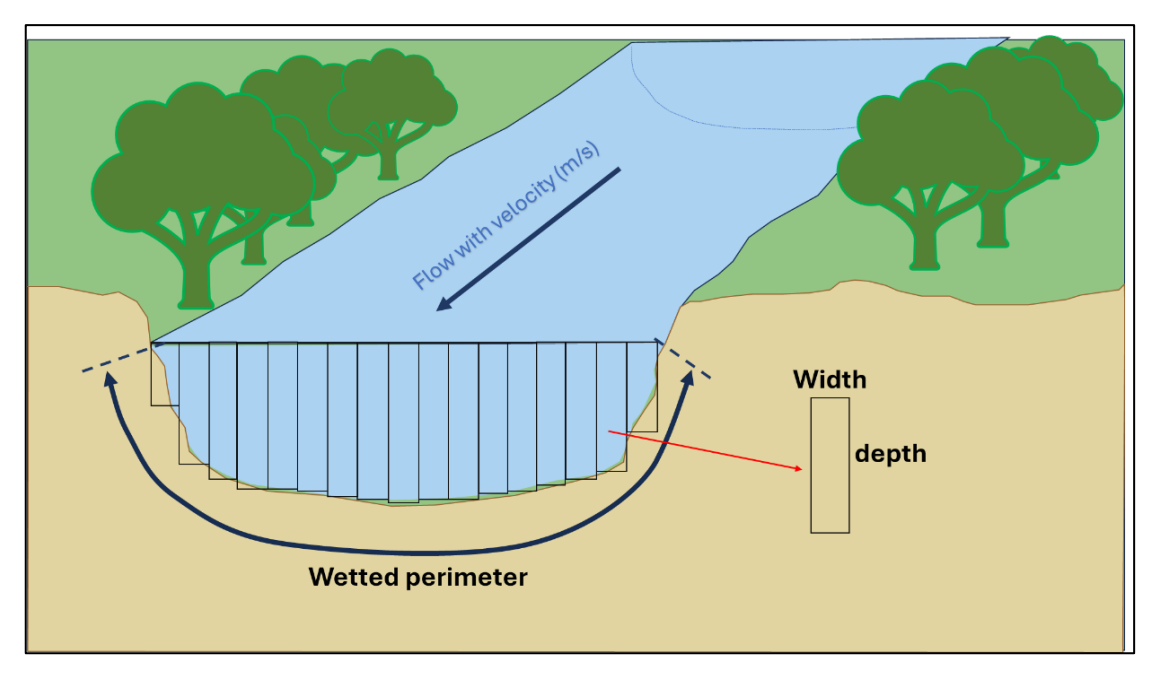


**Figure 19** Stream Discharge calculation total stream discharge developed based on USGS

The initial wetting of the streambed profile significantly contributes to the overall seepage loss. (Blasch et al., 2004). Field surveys indicated mostly a trapezoidal channel geometry (Figure 20). Key parameters, including bottom width, flow depth and side slope, were measured in the field to calculate several estimates using this geometry. With those measures, wet perimeters were calculated to define the contact zone between surface water and groundwater. The estimates are important to investigate water infiltration from the stream into the aquifer. For example, a lower wet perimeter in a deep channel causes less water contact with the bed and bank and results in a lower potential for GW-SW exchange. A greater estimate in a wide and shallow channel, vice versa, has more water contact area, slower flow and promotes potential for seepage (i.e. higher GW-SW interaction). In addition, cross-sectional flow area and hydraulic radius were calculated to estimate streambed conductance, which monitors the recharge from the creek into the aquifer observed from the model simulation. These hydraulic metrics are essential for understanding infiltration dynamics:

Wetted Perimeter Equation (P):

$$P = b + 2\sqrt{y^2 + (zy)^2} \pi r^2$$
 (1)

Cross-sectional Area of Flow (A):

$$A = by + zy^2 \tag{2}$$

 Hydraulic radius (R): ratio of the wetted cross-sectional area (A) to the wetted perimeter (P):

$$R = A \div P \tag{3}$$

Which

y is the water depth (m)

z is the horizontal distance for 1 m vertical distance (m)

b is the bottom width of the channel (m)

B is the width of the water surface (m)

 $\lambda$  is the wetted length measured along the sloped side (m)

 $\alpha$  is the angle of the sloped side from vertical.

The side slope also often specified as a horizontal-to-vertical ratio = z:1

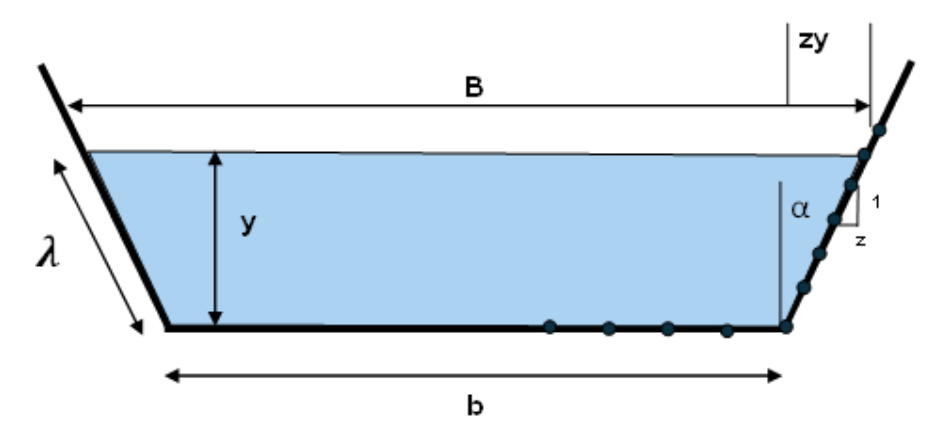
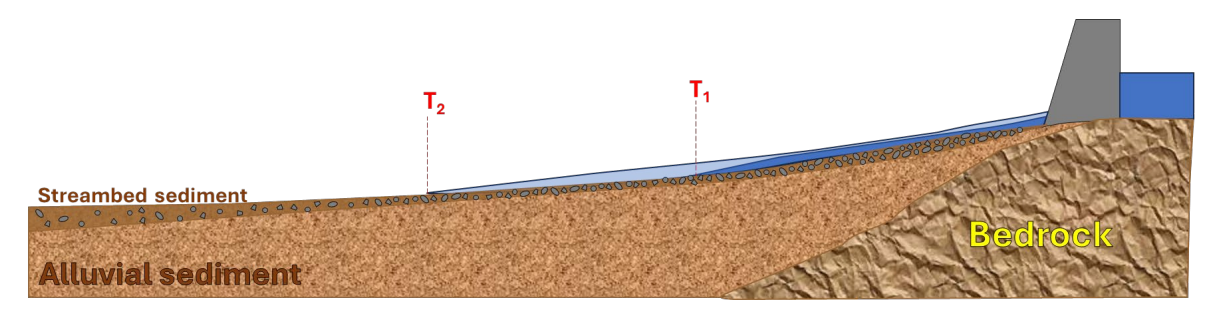


Figure 20 Wetted perimeter parameters in trapezoidal channel geometry.

#### 3.3 Water arrival observation

To assess the propagation of the flow pulse from the environmental water release, water arrival times were recorded at selected locations along Baroota Creek (Figure 21). This observational technique, known as floodwave front tracking, allowed estimation of the flood front velocity and highlighted infiltration-induced delays between upstream and downstream, especially in ephemeral streams where infiltration strongly influences flow continuity (Shanafield and Cook, 2014). During the water released on 22–25 August 2024, field observations were used to determine the first visible presence of surface water at each accessible point (Figure 22). Once the earliest arrival was recorded approximately 1.4 kilometres downstream from the Baroota Reservoir, we observed the timing of flow arrival at five more arrival points downstream using manual logging and georeferencing with GPS-enabled smartphones (Figure 23). The observed arrival times were involved in calibrating the numerical model, particularly contribute to streambed hydraulic conductivity (Ks) adjustment in each stream segment when continuous discharge or stage records were absent in our study (Noorduijn et al., 2014, Hatch et al., 2010).



**Figure 21** Floodwave front tracking. Water arrival times were recorded at each point along Baroota Creek following the environmental water released.

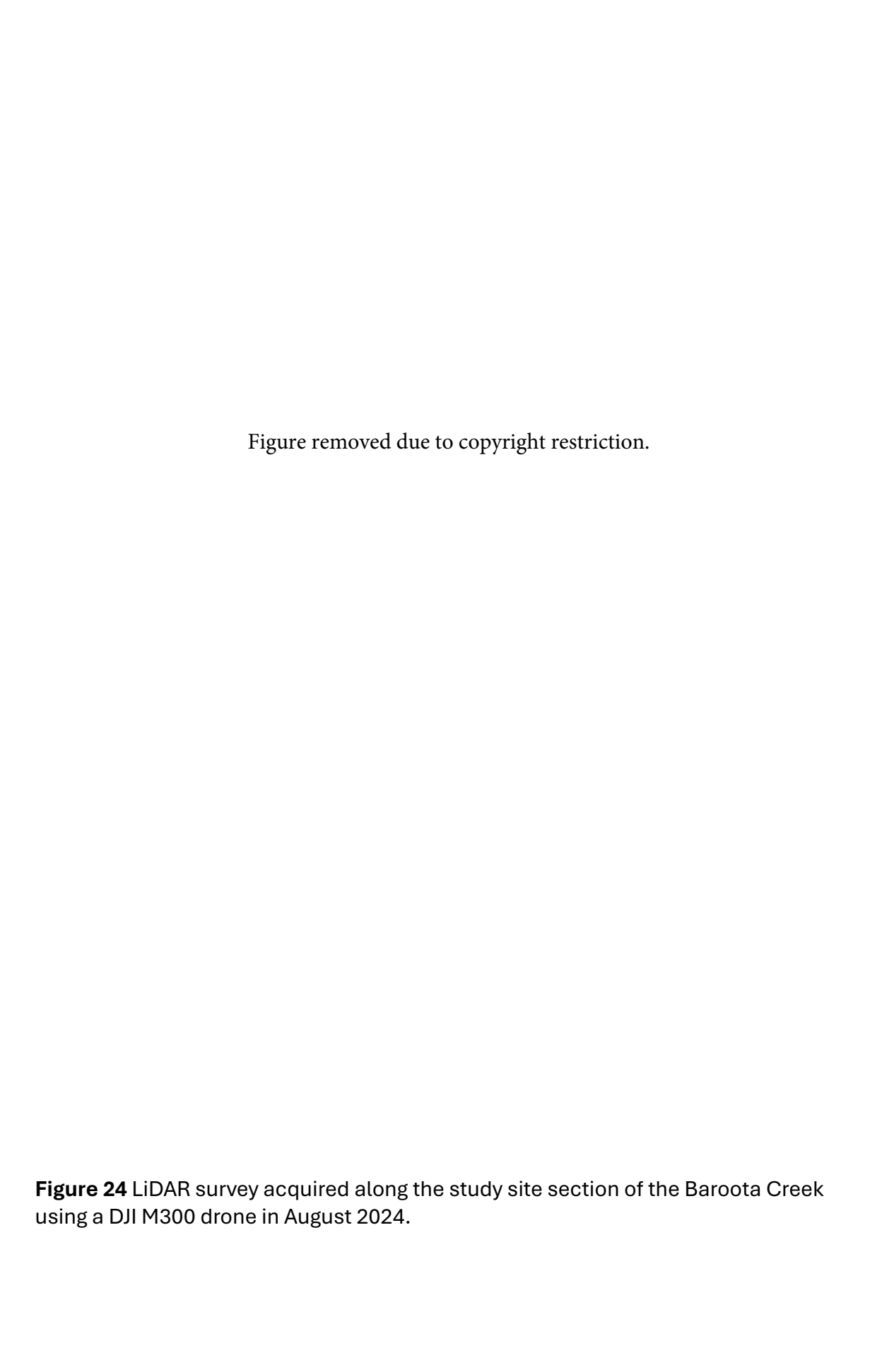


**Figure 22** Flood front observations in the Baroota Creek area during the environmental water released in 22–25 August 2024.

Figure removed due to copyright restriction. Figure 23 Map showing the locations of floodwave front tracking along Baroota Creek during the August 2024 environmental water release. Surface water was released from Baroota Reservoir at approximately 4:00 pm on 22 August 2024.

# 3.4 Light Detection and Ranging Survey (LiDAR)

To generate a high-resolution elevation model of the Baroota Creek corridor Light Detection and Ranging (LiDAR) data were acquired and processed to support spatial discretisation in the numerical model (Figure 24). The LiDAR-derived digital elevation model (DEM) was essential for accurately defining the surface topography of the creek bed and the survey was completed prior to the environmental flow release.



#### 3.5 Conceptual Model of Ephemeral Baroota Creek

The complexity of the groundwater system is simplified during conceptualisation to enable simulation of its key hydrological behaviours. (Barnett et al., 2012). A typical method for modeling groundwater-surface water interaction involves depicting the streambed as a uniform geological structure, with hydraulic properties determined through model calibration (Irvine et al., 2012). In this study, the model was designed to be computationally efficient while retaining the essential interactions between groundwater and surface water. The model aims to estimate the spatial variability of seepage induced by streambed heterogeneity, based on observed variations in streamflow-front velocities along initially dry channel reaches.

Baroota Creek, which is naturally meandering, was simplified into five straight segments for the purpose of modelling. The region is underlain by a substantial thickness of Quaternary alluvial and fluvial sediments, consisting of clays, silts, sands, and gravels deposited as outwash from the Flinders Ranges. In the Baroota area, groundwater is primarily extracted for irrigation from highly permeable gravel beds within these Quaternary deposits, which extend to depths of approximately 100 m (DEW, November 2020). Conceptually, the creek receives intermittent flow from managed environmental releases and typically behaves as a losing stream, particularly during dry periods when the water table is deep. During these events, infiltration through the streambed acts as the dominant mechanism for groundwater recharge. The conceptual model also incorporates the influence of streambed heterogeneity and topographic slope on infiltration. Based on field investigation and hydrogeology data, upstream segments characterised by coarser alluvium and steeper gradients were expected to show higher infiltration rates. In contrast, downstream reaches with finer or compacted sediments and flatter topography were anticipated to have lower seepage potential (Figure 25).

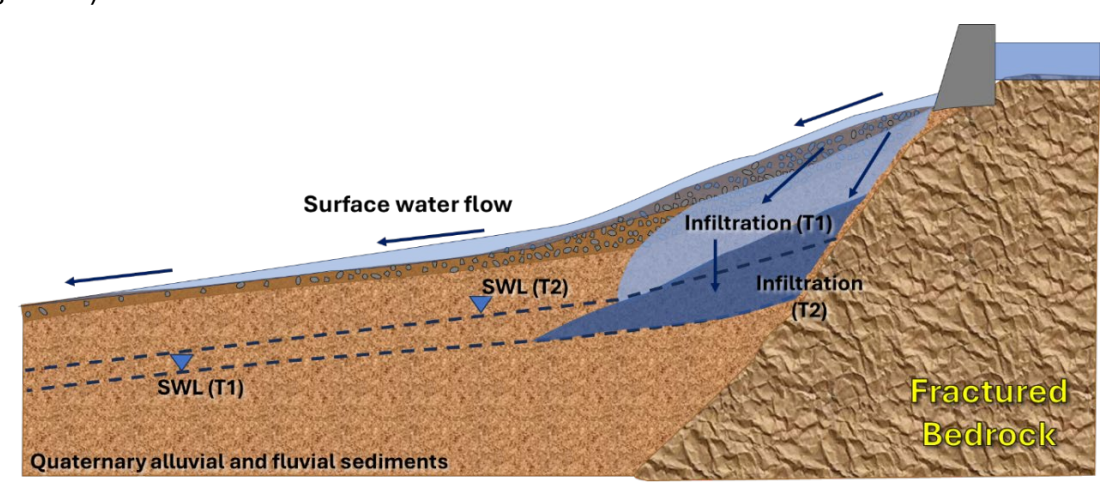


**Figure 25** Conceptual model of GW-SW interaction in Baroota creek area, South Australia.

### 3.6 Modelling Interface

Floodwave routing models of various complexities have been used in studies based on ephemeral rivers (Shanafield and Cook, 2014). Our study employed MODFLOW-NWT to develop a numerical model. The interface, which applies a Newton-Raphson approach simulating groundwater flow under non-linear condition (e.g. drying and

rewetting in unconfined aquifers) (Niswonger et al., 2011), incorporates the Upstream Weighting (UPW) scheme to keep dry cells numerically active, enabling simulation of stream—aquifer exchange even in partially saturated conditions (Lu et al., 2024). This modelling interface enhances the stability of simulation of our numerical model, especially in ephemeral stream systems where surface water often becomes disconnected from the water table (Hunt and Feinstein, 2012). To simulate the advance of the streamflow event, we followed the protocol in Shanafield et al. (2014) to develop the numerical model using a bespoke stream routing package, which applies a diffusion wave appropriate for channel with mild slopes coupled to the Phillips' infiltration equation. This allowed calibration of the streambed hydraulic conductivity using floodwave front tracking and surface water gauging data, enabling more realistic simulation of infiltration and recharge patterns during the environmental flow event.

#### 3.7 Model Setup

The model grid was structured with one unconfined aquifer layer, comprising a single row aligned longitudinally with the stream channel and 69 columns, spanning a total length of approximately 3,450 meters to match the simplified stream segments (Table 1). Each model cell is 50m x 100 m in dimensions, with a 100 m uniform vertical thickness. No-flow boundary conditions were assigned to both lateral edges and the upstream end of the model domain, assuming negligible lateral groundwater inflow. Cells located beneath and directly adjacent to the channel were specifically assigned hydraulic properties to simulate groundwater- stream interactions, enabling a focused infiltration dynamics assessment during the environmental flow release.

The modelled stream length was conceptually divided into 5 segments, which correspond to specific floodwave observation points (Table 1). Streambed elevations were derived from a combination of sources to ensure high spatial accuracy across the model domain. These included GPS measurements collected at the seven stream gauging points, the high-resolution LiDAR-derived Digital Elevation Model (DEM), and a supplementary elevation dataset extracted from Google Earth. This multi-source approach was critical because the precision of the DEM is limited in capturing fine-scale channel incision, the same as the narrow width of Baroota Creek and dense riparian vegetation. Model elevations ranged from 94 mAHD upstream to approximately 50 mAHD downstream, and the slope in the initial two upstream segments was, notably, significantly steeper than the comparatively flatter downstream sections (Figure 26).

**Table 1**. Identified stream segments along Baroota Creek.

Segment	Distance (m)	Number of cells	Cell length (m)
1	338.04	5	67.60
2	787.47	12	65.62
3	793.24	14	56.66
4	440.9	8	55.11
5	1464.63	29	50.50

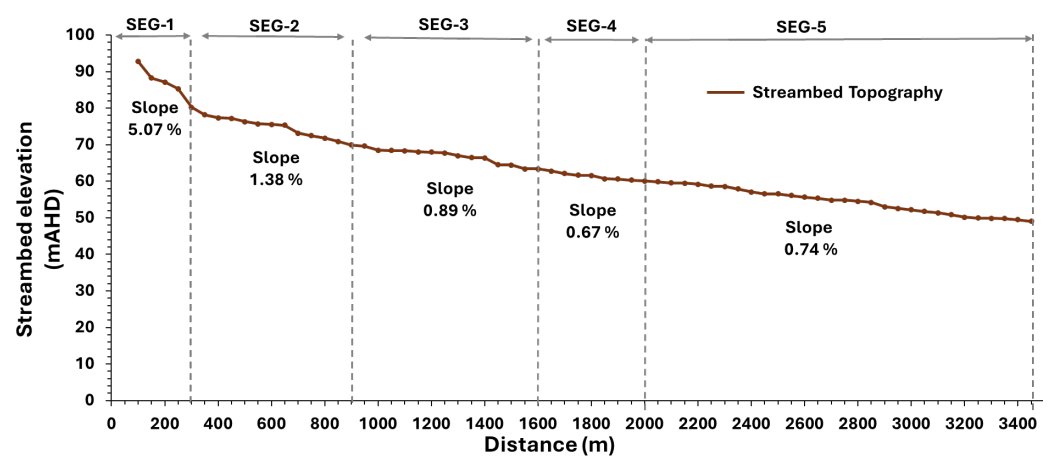


Figure 26 Baroota Creek streambed profile and delineation of stream segments.

To simulate our numerical model, we applied the dfw package developed by Shanafield et al. (2014) to simulate stream aquifer interaction along Baroota Creek. The package, which has similar inputs to the SFR2 package (Streamflow Routing Package version 2), combines diffusion-wave approximation to Saint-Vanant equation with infiltration equation and integrates surface water components into MODFLOW (Shanafield et al., 2014). When considering inputs into MODFLOW, it was noted that the hydraulic properties assigned to the model were based on typical values for unconfined aquifers composed of sandy and gravelly alluvial sediments. The aquifer horizontal hydraulic conductivity was assumed to be equal to the streambed vertical hydraulic conductivity (Ks), both set at 1x10 <sup>5</sup>m/s (Domenico et al., 1998). The General Head Boundary of groundwater level was applied as 0.95 mAHD entering the study area. The specific yield (Sy) was assumed to be 0.15, consistent with values reported for unconfined aquifer composed with medium sand (Fetter, 2001). For the physical criteria of streambed, we set the streambed conductance at 0.35 m<sup>2</sup>/s. Also, the initial volumetric water content and residual moisture content, used in the Brooks-Corey equation for estimating streambed hydraulic conductivity, were set as 0.08 and 0.02. These values fall within the expected range for variably saturated, coarsegrained alluvial materials at the aquifer. Geometric parameters, including wetted perimeter, channel width, and hydraulic radius, were derived from trapezoidal cross-sections based on field-surveyed channel profiles (Akan and Iyer, 2021). Manning's roughness coefficient (n) was assigned as 0.03, which is consistent with shallow, natural channels having low vegetation density and moderately rough beds (Brunner, 2010, Chow, 1959).

### 3.8 Simulation Period and Initial Conditions

The simulation began with a steady-state period under no-flow conditions to establish initial hydraulic constant. The transient simulation was designed to capture the short-term hydrologic response of the system during the environmental water release event. A total of 18 stress periods were defined to represent the full 67,3260 seconds (7.6 days) duration of the flow event (Appendices). Most stress periods were assigned 30 minutes time steps to provide sufficient temporal resolution, while shorter intervals were introduced around observed flow arrival times to more precisely replicate flood wave propagation and infiltration timing. This time-stepping configuration enabled the model to capture the dynamic exchange between groundwater and surface water during periods of

rapid infiltration. It also provided the temporal resolution for calibrating streambed conductance and matching the spatial variability observed in water arrival patterns.

#### 3.9 Calibration and Simulation Scenarios

Our study conducted two scenarios involved in our model calibration which aimed to accurately reproduce the observed arrival times of the floodwave at downstream segments. Both scenarios used identical initial conditions, stream geometry, and model configuration (Figure 27). The differences in input discharge allowed comparison of infiltration behaviour, groundwater response, and stream-aquifer connectivity under contrasting flow volumes.

**Scenario 1**: represented the flow condition based on stream gauging measurements taken at the upstream point during the flow event. The estimated discharge was 1.32 m<sup>3</sup>/s or 114.05 ML/day. This flow was constant for all cross sections and stress periods.

**Scenario 2:** simulated a flow condition based on release data recorded by SA Water in monitoring the successive water level in the Baroota Reservoir. In this case, the total release volume was 560.00 ML, equivalent to 73.68 ML/day, with an average discharge of 0.85 m<sup>3</sup>/s. This flow was constant for all cross sections and stress periods.

In both scenarios, the applied discharge was held constant across all stream cross-sections and stress periods. This simplification was necessary due to limited continuous flow measurements along the channel. Additionally, streambed hydraulic conductivity (Ks) values were adjusted in defined zones along the channel by adopting a floodwave front threshold of 0.01 m³/s. This represents the discharge at which a model cell is considered saturated and capable of transmitting flow to the next downstream segment. To evaluate infiltration and groundwater response under varying surface water conditions, the model was run using each scenario at 7.6 days covering the environmental water release duration from the Baroota Reservoir. The resulting groundwater levels were compared to observe trends and conceptual expectations (Shanafield et al., 2014, Noorduijn et al., 2014).

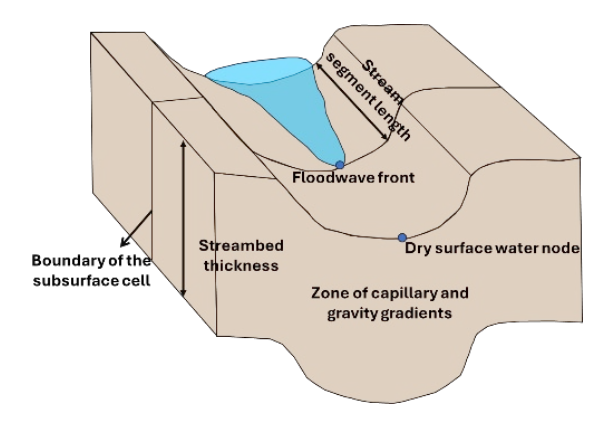


**Figure 27** Conceptual Diagram for Floodwave Front Calibration in MODFLOW (Adapted from Noorduijn et al., 2014).

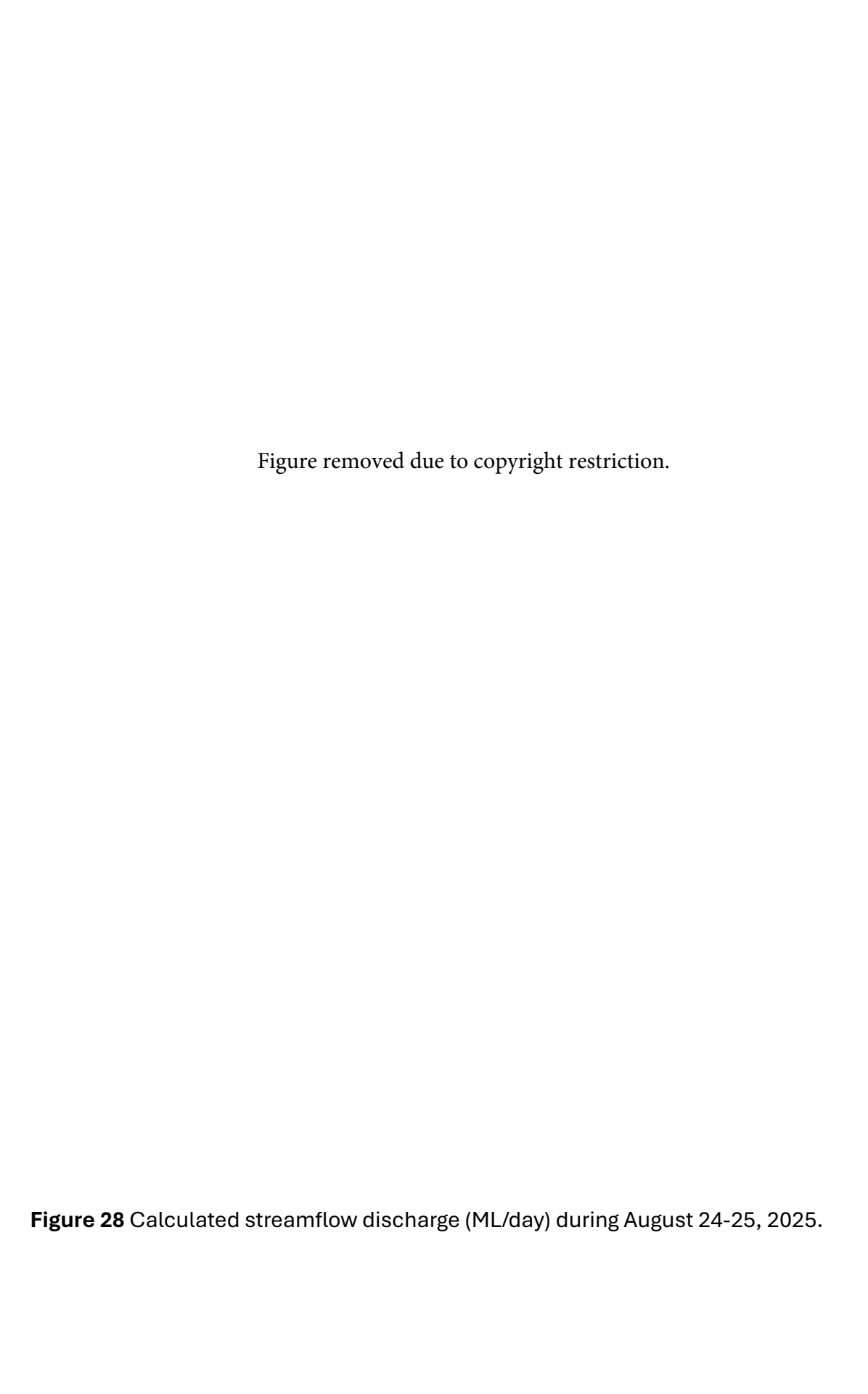
#### 4 Results

# 4.1 Flow Gauging

Discharge measurements began at the upstream station SW-5, which is located at the top of the study area, approximately 1.2 km downstream from the reservoir. The furthest downstream point measured was SW-7, located approximately 2.7 km from the reservoir. The highest discharge was recorded at SW-5, with a flow rate of 1.32 m³/s or 114.05 megalitres per day (ML/day) (Table 2). The lowest discharge was observed at SW-7 with 0.4598 m³/s or 39.73 ML/day. The discharge noticeably dropped at SW-4, where discharge was measured at 0.2828 m³/s or 24.43 ML/day. Moreover, further downstream discharge continued to decline continuously from SW-3 to SW-7, in which the flow measured ranging from 104 m³/s to 0.459 m³/s (Figure 28).

**Table 2** Flow gauging measurement results at seven cross-sections in the Baroota creek area during 24-25 August 2024

Gauging Station	Date Measuring	Flow (m³/s)	Discharge (ML/day)
SW-5	25/08/2024	1.32	114.05
SW-4	25/08/2024	0.282	24.43
SW-3	24/08/2024	1.104	95.39
SW-2	24/08/2024	1.055	91.20
SW-1	24/08/2024	1.042	90.05
SW-6	24/08/2024	0.858	73.30
SW-7	25/08/2024	0.459	39.73



## 4.2 Creek Geometry and Cross-Sections

Overall, the channel geometry of the Baroota Creek was generally trapezoidal in shape, though some irregularity was observed (Figure 29, Appendices). At the upstream gauging site SW-5, the average water depth was approximately 0.26 m, with a wetted width of about 7 m. Further downstream at SW-7, the cross-section revealed an average water depth of 0.34 m and a wetted width of approximately 9 m. These variations reflect natural changes in channel morphology and may be influenced by sediment deposition, and bank erosion.b

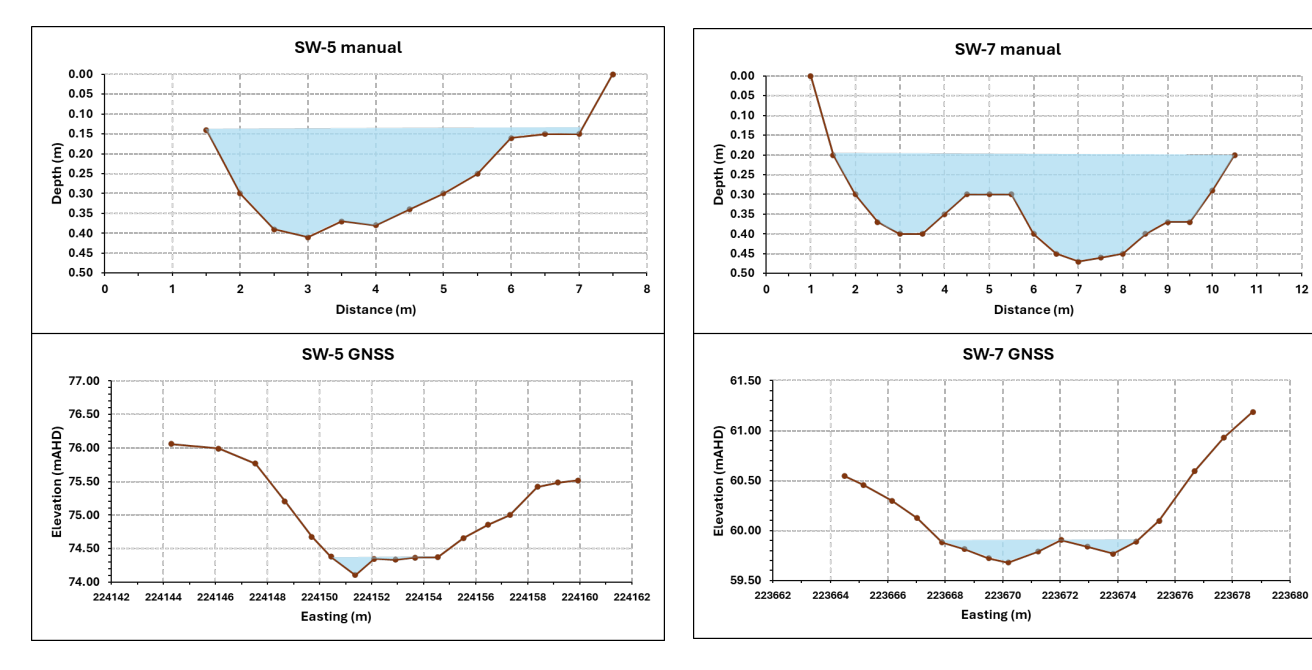


**Figure 29** Comparison of Creek Geometry Derived from Gauging Measurements (Top) and GNSS Data (Bottom).

#### 4.3 Model Results

The model was calibrated by adjusting streambed hydraulic conductivity (Ks) in five defined segments to match observed floodwave arrival times recorded during the August 2024 environmental flow release. Calibration was performed manually using a trial-and-error approach, where Ks values were iteratively adjusted until the simulated floodwave reached the threshold discharge of 0.01 m³/s at the final cell of each segment, consistent with field-observed arrival points.

In Scenario 1, the calibrated streambed hydraulic conductivity (Ks) was higher at Segment 1 at approximately 80 m/day and Segment 2 is about 66 m/day, followed by a sudden decrease on Segment 3 to around 1.2096 m/day (Table 3). The floodwave front tracking at the end of the reach was in the target at 0.01 m³/s across Segment 3 to Segment 5 while noticeably higher at Segment 1 (0.9679 m³/s, 83,626.6 m³/day) and Segment 2 (0.04229 m³/s, 3,653.86 m³/day).

For the simulated flow into the creek, the initial streamflow was set at 114,048 m³/day, based on field discharge measurements from gauging station SW-5 (Figure 30). Surface water travelled approximately 300 m downstream within the first 2 hours and 54 minutes, reaching the second gauging observation point. During this interval, the

simulated flow decreased from 114,048 m³/day to 83,626.56 m³/day. At Segment 2, the flow continued an additional 600 m downstream, reaching the third observation point after 18 hours and 29 minutes. The surface water volume dropped significantly from 114,048 m³/day at the upstream boundary to 3,653 m³/day. By the time flow reached the fourth observation point, located approximately 700 m beyond Segment 2 with after 52 hours and 31 minutes, the simulated volume had reduced further to 865 m³/day. Despite continuing another 1,850 m downstream to the fifth and final observation point until 187 hours, the simulated streamflow remained stable at approximately 865 m³/day.

For the total stream leakage, the measure in Segment 1 was at 36,781 m³/day, with the highest leakage rate (~11,000 m³/day) occurring at 150 m distance within the first 2 hours and 54 minutes (Figure 31). Over time, the total leakage at Segment 2 increased to 113,167 m³/day by 18 hours and 29 minutes into the simulation. In contrast, Segments 3 to 5 exhibited negligible leakage. By the time after 52 hours and 31 minutes, the after flow had reached Segment 3 having 113,222 m³/day of total leakage, virtually unchanged by the end of the simulation at 187 hours (7.79 days) water flow distance 3,450 m, where the final leakage was 113,189 m³/day.

Although the aquifer properties were not calibrated in this study, groundwater response is noted but not expected to match observed water levels precisely but provided a useful starting point for future model refinement. In Scenario 1, the simulated groundwater head response showed an increase from the initial head (0.95 mAHD) to approximately 1.8 mAHD at the upstream at 300 m after around 3 hours of flow event. As flow continued further downstream at 900 m (Segment 1 and Segment 2), the water table rose to approximately 6.0 mAHD after approximately 18.5 hours, whereas groundwater response became minimal further downstream from 900 m to 3,450 m. At the end of the simulation period (187 hours), the maximum simulated groundwater head was observed at 450 m, where it reached approximately 53 mAHD (Figure 32).

Similar in Scenario 2, calibrated streambed hydraulic conductivity (Ks) values were higher at the first two segments (Segment 1: 55 m/day, Segment 2: 45 m/day) while that of the rest of the segments were low (> 0.4 m/day. Also, the target of waterfront flood at the end of the reach is higher at the first two segments (Segment 1:  $0.6233 \, \text{m}^3/\text{s}$ , Segment 2:  $0.04518 \, \text{m}^3/\text{s}$ ) while it remained stable across the rest of the segment ( $0.01002 \, \text{m}^3/\text{s}$ ). These results followed the same general trend as Scenario 1, with higher Ks values in the upstream segments and lower downstream values) (Table 4).

The simulation exhibited a similar trend to Scenario 1, though with lower overall discharge values (Figure 33). In Segment 1, flow dropped from 71,887 m³/day to 53,853 m³/day, followed by discharge reduced further to 3,903 m³/day at Segment 2, corresponding to an 11% loss. Across Segments 3 to 5, streamflow stabilized at 865 m³/day, also representing about an 11% loss.

Scenario 2, which had a lower initial flow rate showed a total leakage of 22,261 m<sup>3</sup> at Segment 1, again peaking around 150 m at 2 hours and 54 minutes (Figure 34). Leakage continued into Segment 2 with a cumulative volume of 70,031 m<sup>3</sup> by 18 hours and 29 minutes by 900 m. Like in Scenario 1, Segments 3 to 5 exhibited minimal leakage. For instance, at 52 hours and 31 minutes, total leakage had reached 70,883 m<sup>3</sup>. The leakage slightly decreased to 70,851 m<sup>3</sup> at 3,450 m by the end of the simulation.

The groundwater head response in this scenario increased to around 1.5 mAHD from its initial level, followed by a further increase to 4 mAHD when reaching the next segment (at 900 m). Same as Scenario 1, the response was steadily low between 900m and 3,450 m. As the simulation period reached 187 hours, the maximum groundwater head reached 36 mAHD at around 450 m (Figure 35).

**Table 3** Simulated streambed hydraulic conductivity (Ks) in model calibration in Scenario 1.

Segment	Streambed hydraulic conductivity (Ks) (m/s)	Streambed hydraulic conductivity (Ks) (m/day)	Flow into stream at the end of the reach (m³/s)	
1	0.00092	79.488	0.9679	
2	0.00076	65.664	0.04229	
3	0.000014	1.2096	0.01001	
4	0.000007	0.6048	0.01001	
5	0.000009	0.7776	0.01001	

**Table 4** Simulated streambed hydraulic conductivity (Ks) in model calibration in Scenario 2.

Segment	Streambed hydraulic conductivity (Ks) (m/s)	Streambed hydraulic conductivity (Ks) (m/day)	Flow into stream at the end of the reach (m <sup>3</sup> /s)	
1	0.00064	55.296	0.6233	
2	0.00052	44.928	0.04518	
3	0.000035	3.024	0.01047	
4	0.000005	0.432	0.01002	
5	0.0000085	0.7344	0.01002	

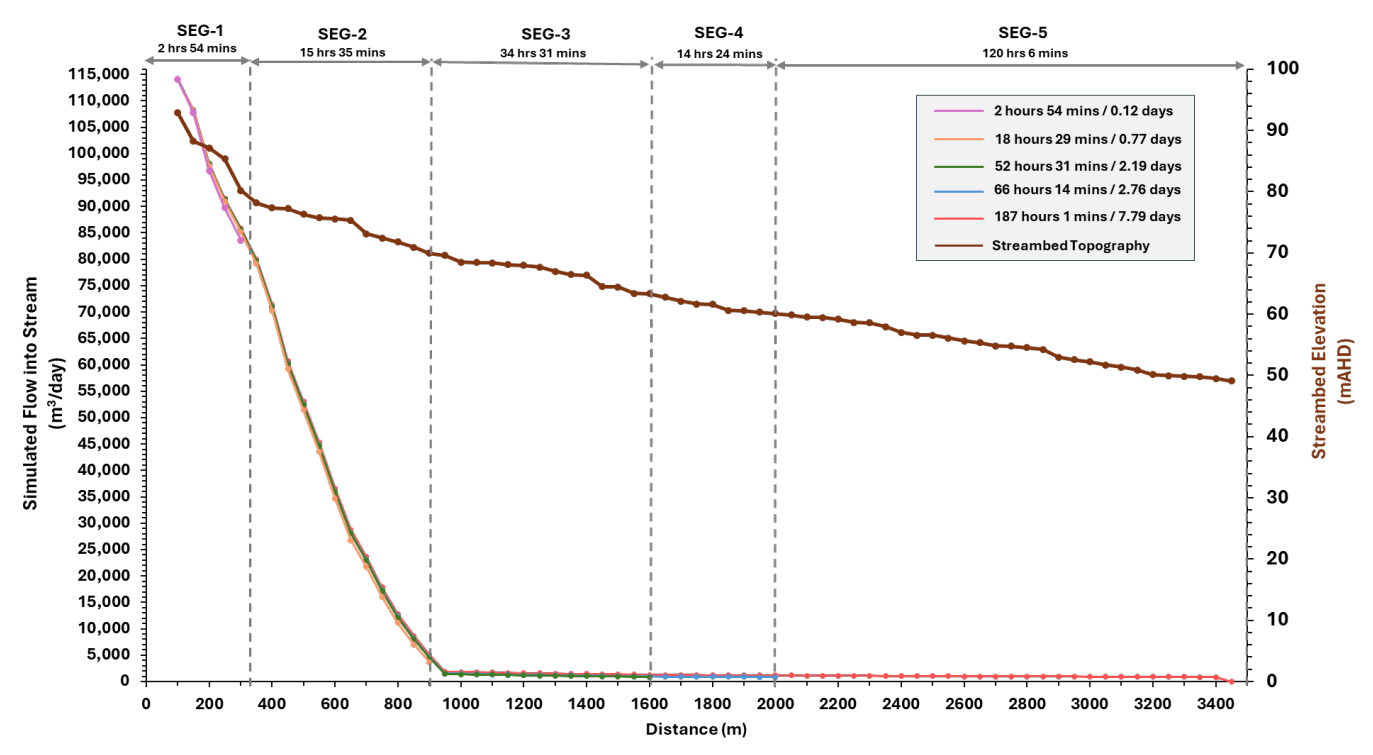


Figure 30 Simulated flow in the creek with initial discharge 114,048 m<sup>3</sup>/day (Scenario 1).

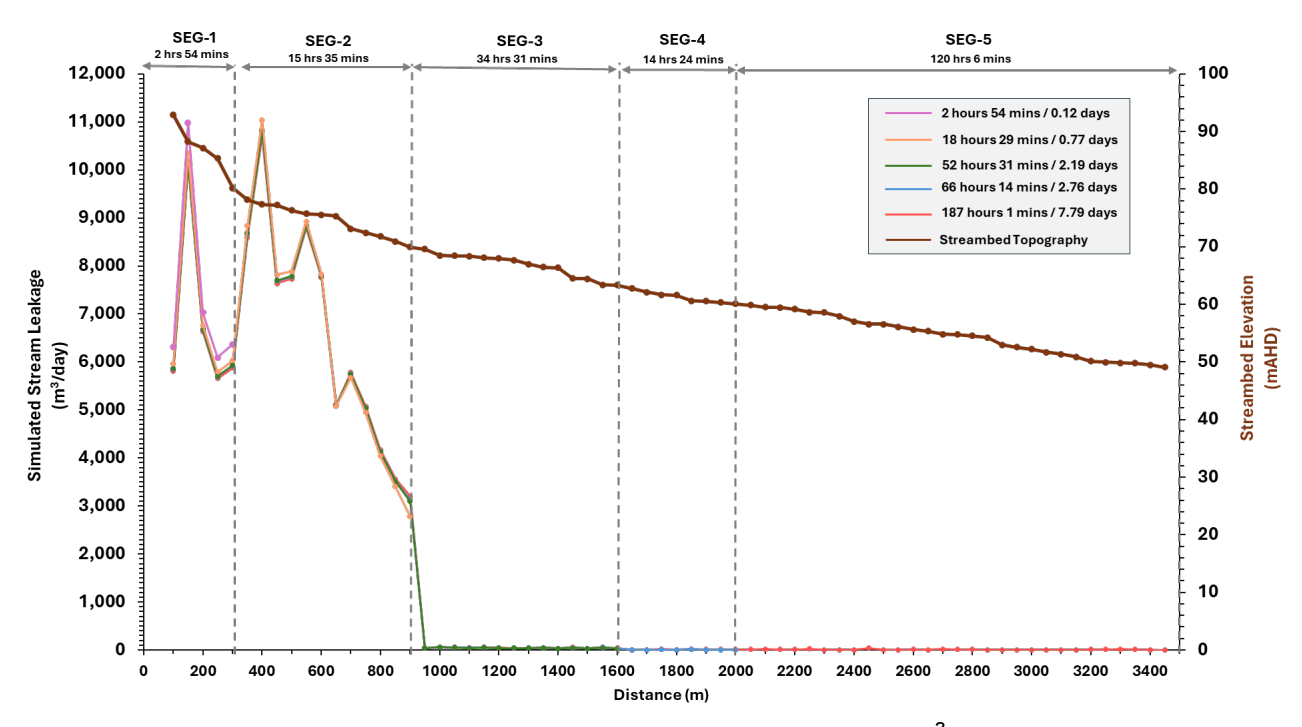
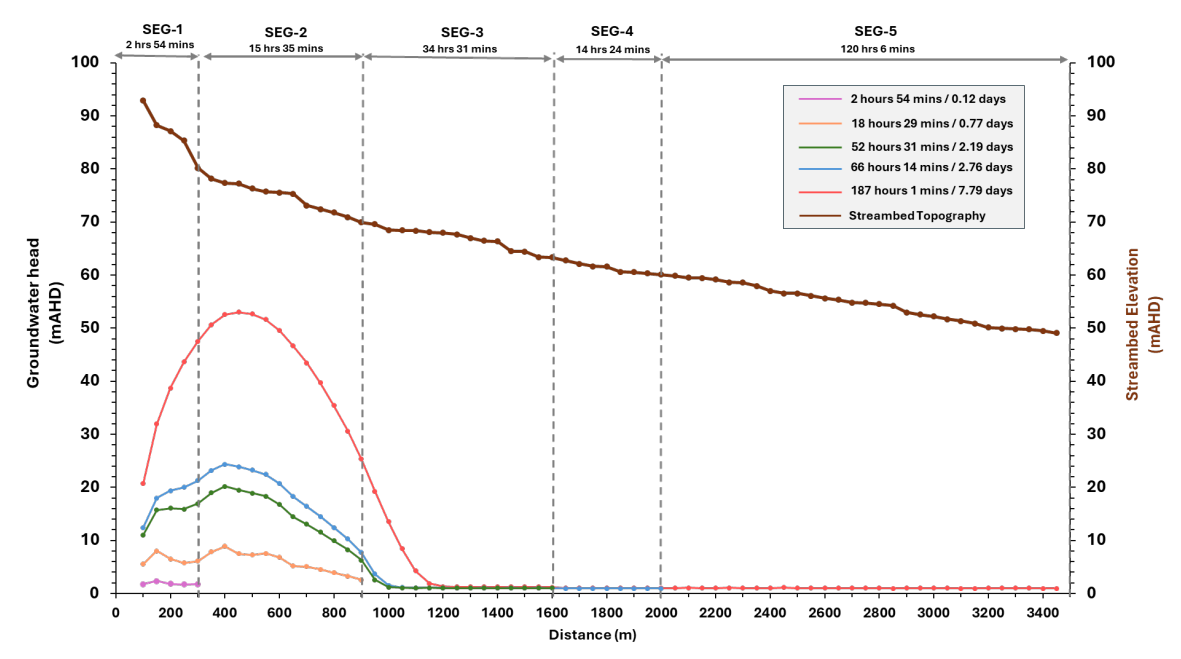


Figure 31 Simulated stream leakage with initial discharge 114,048 m<sup>3</sup>/day (Scenario 1).



**Figure 33** Simulated groundwater head responding initial discharge 114,048 m<sup>3</sup>/day (Scenario 1).

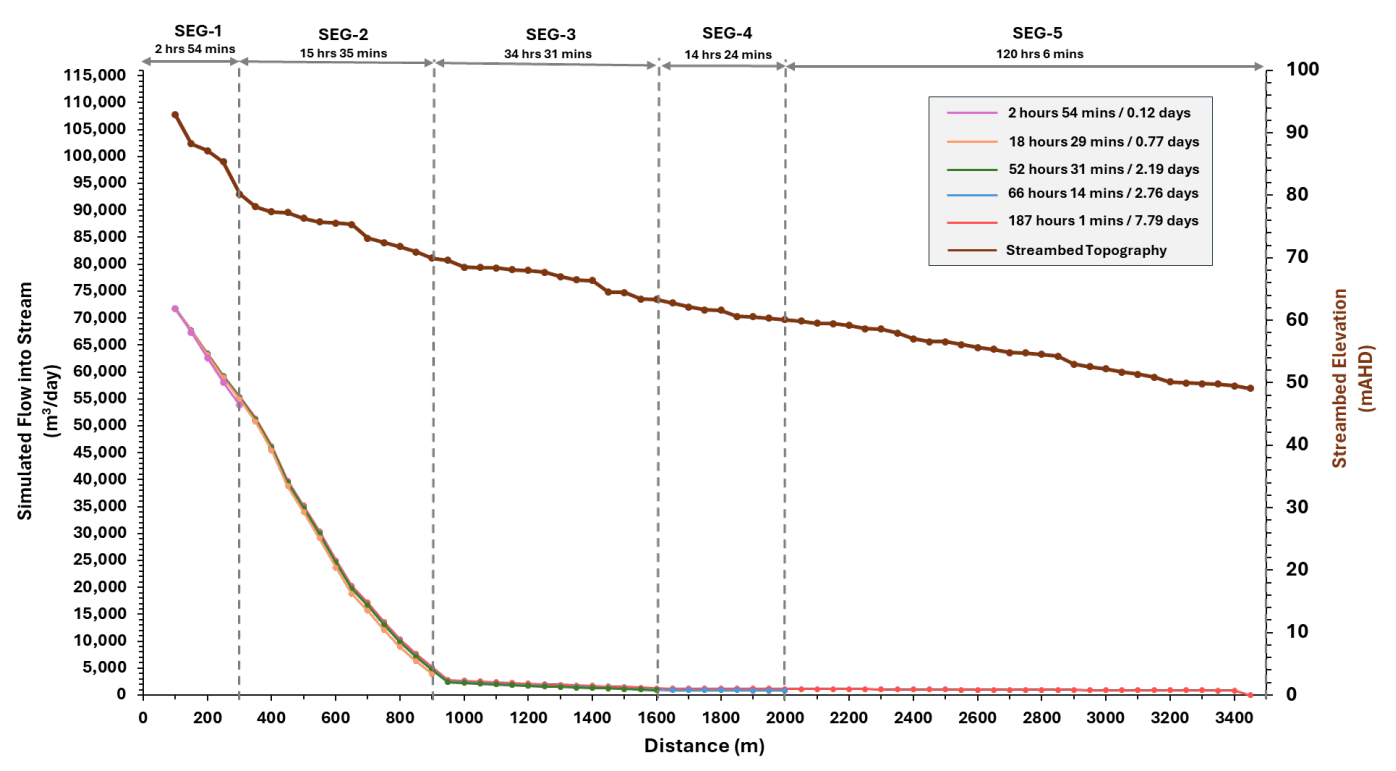


Figure 32 Simulated flow in the creek with initial discharge 71,887 m<sup>3</sup>/day (Scenario 2).

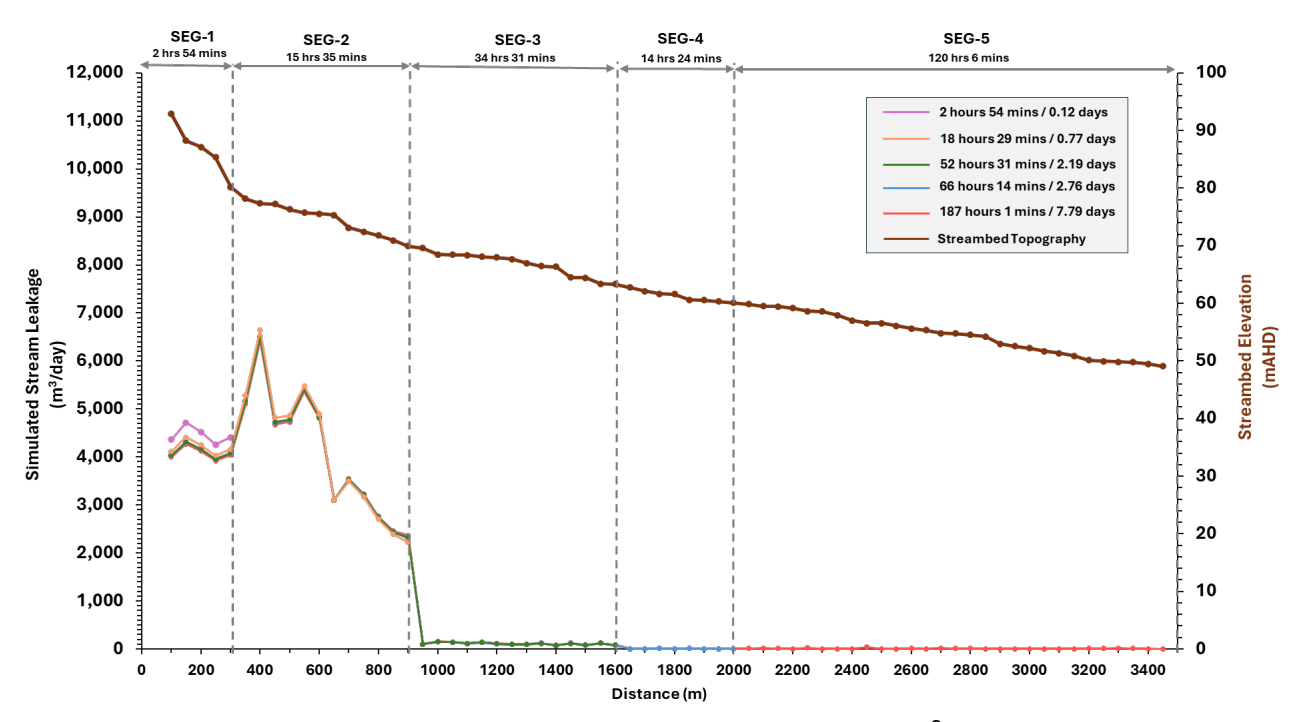
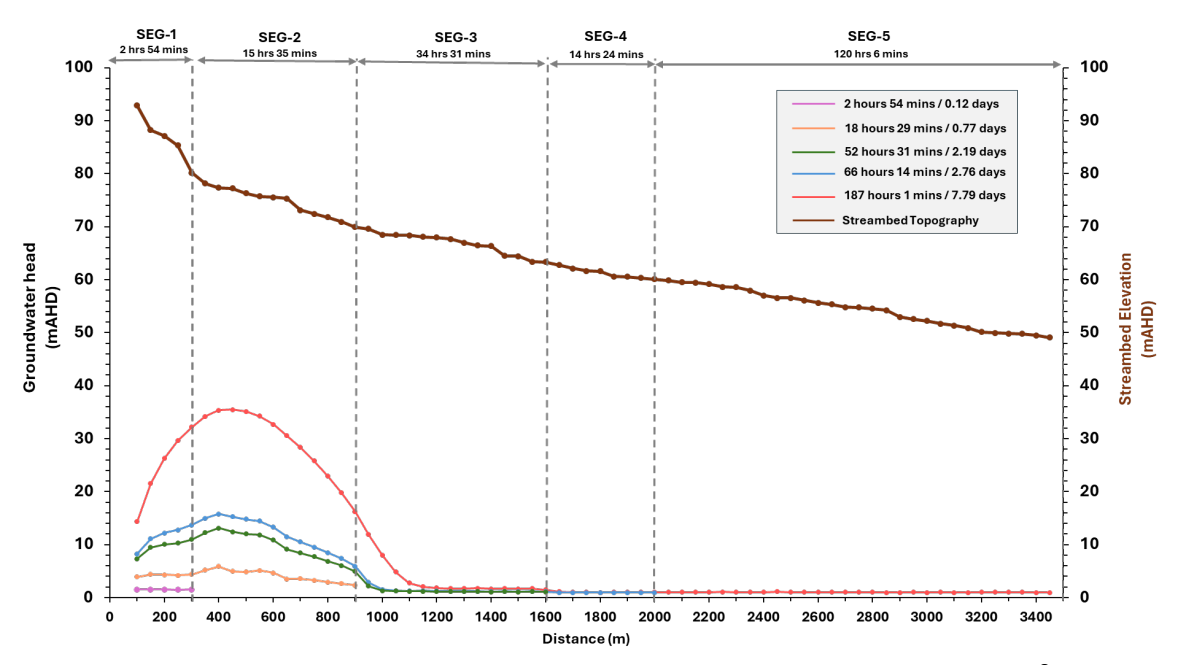


Figure 34 Simulated stream leakage with initial discharge 71,887 m<sup>3</sup>/day (Scenario 2).



**Figure 35** Simulated groundwater head responding initial discharge 71,887 m<sup>3</sup>/day (Scenario 2).

#### 5 Discussion

This study employed numerical groundwater modelling using MODFLOW-NWT to investigate GW-SW interactions within the Baroota Creek, an ephemeral watercourse in a semi-arid region. Two simulated flow scenarios, based on different inflow rates, were used to assess infiltration dynamics, spatial variability of streambed hydraulic conductivity (Ks), groundwater head responses, and the influence of streambed topography. The findings provide insights on understanding recharge processes in ephemeral streams by acknowledging that soil type, unsaturated zone dynamics and topography are the key factors on controlling streamflow generation and infiltration in non-perennial systems (Brunner et al., 2009, Gutierrez-Jurado et al., 2021).

Ephemeral streams in semi-arid regions present distinct hydrological challenges. Characterized by shallow soils, low water storage capacity, and limited connection to regional aquifers, these systems often lack baseflow and remain dry for much of the year (Levick et al., 2008, Koch et al., 2020). These characteristics, including the ephemeral nature and limited connection to a regional aquifer, were also defining the features of Baroota creek system investigated in this study. Differentiating infiltration from actual aquifer recharge is critical. Our methods based mainly on streambed properties and streamflow observations typically overestimate recharge by neglecting transmission losses and the lag time between infiltration and aquifer response (Shanafield and Cook, 2014). Moreover, transmission losses can be highly variable, with factors such as antecedent moisture, channel morphology, and sediment clogging influencing the degree of infiltration (Shanafield et al., 2012).

In this study, the primary focus was on understanding the dynamics of infiltration within Baroota creek streambed rather than quantifying regional aquifer recharge. However, numerical modelling approach developed by Shanafield et al., 2014 possesses the capability to simulate both infiltration and estimate streambed saturated hydraulic conductivity (Shanafield et al., 2014, Noorduijn et al., 2014). While streambed infiltration during flood events is considered a significant mechanism for aquifer recharge in arid regions, accurately quantifying recharge from ephemeral rivers continues to pose a challenge. Consequently, while our models focused on the infiltration process, the methodology could be extended to capture regional aquifer recharge if more extensive hydrogeological data were obtainable (Villeneuve et al., 2015, Shanafield et al., 2014).

We acknowledge that a segment-by-segment water balance, showing cumulative infiltration volumes from each stream segment, would have strengthened the interpretation of flow losses and spatial variability. This information could have been derived from model cell-by-cell budget outputs or zone-based analysis of cumulative leakage over time. However, limitations in post-processing configuration and model output extraction prevented detailed volumetric estimates in this study.

## 5.1 Model Evaluation Against Field Observations

Flow gauging during the 24–25 August 2024 environmental flow release provided point-in-time discharge measurements rather than cumulative totals. For example, discharge at SW-5 was 1.32 m<sup>3</sup>/s (114.05 ML/day), decreasing to 0.459 m<sup>3</sup>/s (39.73 ML/day) at SW-7. This spatial decline indicates substantial infiltration losses,

consistent with modelled leakage patterns, and supports the conceptualisation of Baroota Creek as a strongly losing stream. Such patterns are consistent with previous studies in arid and semi-arid environments where transmission loss dominates the water balance (Levick et al., 2008). Simulated floodwave arrival discharges presented in Table 3 were calibrated to match the threshold of 0.01 m³/s; deviations from this value were interpreted as calibration error.

Incorporating streamflow gauging results as upstream boundary conditions and calibrating the model against observed surface flows enabled robust estimation of seepage fluxes. Specific yield was identified as one of the most influential aquifer parameters affecting the magnitude and timing of simulated groundwater response (Noorduijn et al., 2014). Despite several limitations acknowledged in this study, the modelling approach offers Despite several limitations acknowledged in this study, the modelling approach demonstrates strong potential for assessing the longitudinal variability of seepage fluxes from ephemeral and intermittent streams. Prior research has shown that integrating streamflow and groundwater data improves model calibration and enhances the reliability of seepage estimate (Noorduijn et al., 2014, Niswonger et al., 2005, Brunner et al., 2011).

## 5.2 Streamflow Scenarios and Groundwater Response

To reflect field observations, two uniform discharge scenarios were simulated. Scenario 1 applied streamflow of 1.32 m<sup>3</sup>/s (114,048 m<sup>3</sup>/day), corresponding to flow measured at SW-5. Scenario 2 used a reduced streamflow input of 0.83 m<sup>3</sup>/s, derived from the average release over 7.79 days. Both scenarios targeted a downstream arrival of the wetting front to align with observed flow at the farthest gauging station. The calibrated Ks values ( $>7.6 \times 10^{-4}$  m/s) showed interaction between stream leakage and groundwater, with infiltration concentrated in upstream segments and negligible leakage in downstream segments with low-permeability beds. These calibrated values were consistent with observed discharge loss patterns and groundwater response profiles, further supporting the representation of Baroota Creek as a strongly losing stream. Higher Ks values were simulated in the upstream 0–900 m section, consistent with coarse sand or gravel substrate (Domenico et al., 1998). Downstream reaches exhibited lower Ks, indicative of finer sediments (e.g., silt or clay). This Ks gradient resulted in reduced infiltration and recharge downstream. In both scenarios, the largest streamflow losses occurred in the upstream segment. Leakage rates declined rapidly beyond 900 m, and the system approached steady-state, consistent with previous studies of infiltration patterns observed in arid-zone ephemeral streams (Morin et al., 2009, Shanafield et al., 2012, Noorduijn et al., 2014, Dogramaci et al., 2015)

These results are supported by field and modelling studies, which have shown that streambed sediment composition plays a dominant role in infiltration dynamics, especially in disconnected or intermittent stream systems (Lamontagne et al., 2005). Moreover, changes in Ks can result from sediment compaction, biofilm growth, or clogging during flood events, introducing temporal variability that should be captured in future transient simulations (Batlle-Aguilar and Cook, 2012, Cuthbert et al., 2016).

While a complete water balance analysis was beyond the scope of this study, discharge measurements from gauging stations showed spatial trends consistent with

model predictions. For example, flow decreased from 114.05 ML/day at SW-5 to 39.73 ML/day at SW-7, suggesting significant infiltration losses over the reach. The close alignment between modelled and observed attenuation patterns supports the calibration approach and affirms the stream's losing behaviour.

## 5.3 Influence of Streambed Topography and Aquifer Simplification

Streambed elevation, derived from DEM and field measurements, influenced infiltration patterns. Steeper reaches produced greater hydraulic gradients and thus higher infiltration rates, while flatter reaches yielded lower seepage. These findings align with studies that show streambed slope and morphology significantly affecting hyporheic exchange and infiltration (Boano et al., 2014; Shanafield et al., 2012 (Warix et al., 2023). The morphology of ephemeral creeks, including step-pool sequences and lateral bars, can control local flow paths and the spatial distribution of recharge (Molnar et al., 2010, Rabanaque et al., 2022).

While the model incorporated topographic elevation, the simplified trapezoidal cross-section used for the Baroota Creek may not fully reflect field conditions. The modelled geometry appeared unreasonably narrow and shallow, which likely underestimated the wetted perimeter and thus affected infiltration estimates. In hydraulic modelling, the wetted perimeter is a key parameter for estimating hydraulic conductivity to influence seepage and conveyance capacity (Zhong et al., 2023). Smaller cross-sections with underestimated wetted perimeters may exaggerate infiltration rates due to a reduced contact area between stream water and the streambed (Chow, 1959, Anderson et al., 2015). Future models could incorporate field-derived cross-sectional data to calculate and validate the wetted perimeter along different stream segments, ensuring more realistic representation of hydraulic behaviour (Sophocleous, 2002).

Comparisons between manual and GNSS-derived cross-sections confirmed that GNSS surveying provides a more realistic representation of the creek's shape and variability. While manual measurements offer a practical field method, they rely on simplified assumptions about bed shape and surface slope, which can lead to uncertainty in flow area and streambed slope estimation. The detailed GNSS data collected at these sites not only improved the reliability of flow measurements but also supported the calibration of streambed parameters in the MODFLOW model by providing accurate channel slope, depth, and surface connectivity metrics.

Although the stream channel was simplified to a trapezoidal cross-section, elevation changes were preserved to simulate realistic flow gradients. This approach highlights the importance of accurate topographic representation when modelling stream-aquifer interactions in complex terrains. Given that incision, bank instability, and sediment redistribution are common in dryland streams, future models could benefit from detailed representation of stream form dynamics (Camporeale et al., 2013, Boulton et al., 1998, Wohl et al., 2005).

#### 5.4 Limitations

Potential limitations that may have affected the efficiency and certainty of our model included the short period of field data collection (22–25 August 2024). Both groundwater instrumentation and surface gauging were carried out during the short field period. This limit dedicated time for detailed inflow measurements which constrained the opportunity for more comprehensive and precise data, reducing the temporal resolution of inflow and system response observations.

A significant source of uncertainty in this study is from the creek inflows, which were treated as a crucial boundary condition for the model. Due to limited access to the upstream reach due to its densely vegetated terrain, creek discharge data near the reservoir were not directly captured. Instead, the inflow value of 1.32 m³/s was derived from a gauging conducted at midstream site SW-5 on 24 August 2024, approximately 1.5 days after the environmental water release began. Interestingly, this measured flow rate was higher than what was inferred from the recorded reservoir releases. This value was subsequently used as the primary inflow for the model and for assessing consistency along the channel during streambed hydraulic conductivity (Ks) calibration. While an additional scenario using the recorded reservoir release was employed to explore potential variations, the accuracy of the inflow estimate remains a key limitation of this study.

Finally, the simplification of our numerical model resulted in a limited number of streambed geometry and Ks measurements and thus required interpolation across large sections, potentially masking fine-scale heterogeneity. In reality, streambed properties can vary markedly over short distances, influenced by flow paths, vegetation cover, and geomorphic controls (Ghosh and Pekkat, 2019, Naganna et al., 2017). Streambed roughness characterisation likely introduced some uncertainties in leakage estimation (Shanafield et al., 2014, Min et al., 2020). Noorduijn et al. (2014) applied a uniform Manning's n across their study reach and noted that spatial variability in channel roughness due to bends and vegetation was not accounted for and may have introduced calibration error. While they did not quantify the extent of this impact, it is possible that roughness effects become more significant in areas with high transient infiltration.

## 5.5 Future Directions

To improve model accuracy, future studies should refine topographic detail. High-resolution GNSS surveys can provide reliable checkpoint coordinates to assess the vertical accuracy of LiDAR-derived Digital Elevation Models (DEMs), enabling more precise characterisation of streambed geometry and micro-topography (Aguilar and Mills, 2008). While LiDAR offers broad coverage of the landscape, it can also be used to estimate surface flow discharge and assess channel morphology, particularly in open environments (Biron et al., 2013). Combining GNSS and LiDAR data enhances the spatial resolution of elevation models, which is crucial for capturing fine-scale variations in flow paths and identifying zones of infiltration, ultimately improving the model's predictive performance.

The installation of shallow piezometers along the creek would provide measurements of groundwater levels and the watertable response to the environmental water releases, which would improve the model calibration. Hydrogeophysical methods such as nuclear magnetic resonance (NMR) and electromagnetic surveys could characterise the subsurface conditions and improve the saturated hydraulic conductivity estimates of the creek bed that are used in the model.

Isotope analysis of the surface water, soil water, groundwater and the xylem water of the River Red gums would help trace water sources, flow paths and mixing prior to, during and after the environmental flow event. Pumping tests during flow events could further inform aquifer properties such as specific yield (Sy) and specific storage (Ss) (Batelaan and De Smedt, 2007).

Expanding the model domain and complexity, including vertical layering and broader catchment boundaries, would allow evaluation of cumulative recharge from multiple events or long-term climatic changes. Incorporating unsaturated zone flow and dynamic root uptake models could also help capture evapotranspiration losses more realistically (Maxwell and Kollet, 2008).

Engaging with local stakeholders to communicate model outcomes could support adaptive water management and conservation of riparian vegetation, particularly River Red Gum communities. These groundwater-dependent ecosystems rely on episodic recharge events to sustain moisture in the unsaturated zone (Boas and Mallants, 2022).

#### 6 Conclusion

This study presents a modelling investigation of how environmental flow releases influences streambed infiltration and the impacts to groundwater and surface water interactions in a non-perennial stream in a semi-arid setting. The primary water management objective of the environmental flow release for the Baroota Creek catchment was to provide water and subsequent soil moisture conditions to increase water availability to the riparian vegetation, particularly the River Red Gum woodlands. Field observations and numerical modelling revealed that the creek functions as a losing stream with higher infiltration rates in the upstream reaches, where coarse sediments and steeper creek bed gradients facilitated greater water losses into the subsurface. These streamflow conditions likely contributed to infiltrated surface water to reach the root zones of riparian vegetation. In contrast, the downstream reaches of the creek exhibited finer sediments, lower creek bed gradients, and reduced infiltration, raising uncertainty about whether water from the flow event reached the root zone of the riparian vegetation. Despite model simplifications with limited stream geometry data and measured streambed hydraulic conductivity values, the results captured the spatial variability in infiltration dynamics during the flow event. This work establishes a foundation for future assessments of how environmental flow events can be managed to extend the duration of the flow event and infiltration to improve the riparian ecological functions of non-perennial streams. Integrating higher-resolution cross-sectional surveys and hydrogeophysical data will be essential to improve the extent of the wetted perimeter estimates either side of the creek and seepage accuracy. Ultimately, this study contributes to improving the understanding of recharge mechanisms in ephemeral streams, and provides insight into the effect of environmental flows impacting groundwater-dependent ecosystems. The findings also support culturally inclusive water planning that aligns ecological restoration goals with First Nations values.

### 7 References

- AGUILAR, F. J. & MILLS, J. P. 2008. Accuracy assessment of lidar-derived digital elevation models. *Photogrammetric record*, 23, 148-169.
- AKAN, A. O. & IYER, S. S. 2021. Open channel hydraulics, Amsterdam, Netherlands;, Elsevier.
- ANDERSON, M. P., WOESSNER, W. W. & HUNT, R. J. 2015. *Applied groundwater modeling : simulation of flow and advective transport, Amsterdam, [Netherlands, Academic Press.*
- ARTHINGTON, A. H., BHADURI, A., BUNN, S. E., JACKSON, S. E., THARME, R. E., TICKNER, D., YOUNG, B., ACREMAN, M., BAKER, N., CAPON, S., HORNE, A. C., KENDY, E., MCCLAIN, M. E., POFF, N. L., RICHTER, B. D. & WARD, S. 2018. The Brisbane Declaration and Global Action Agenda on Environmental Flows (2018). *Frontiers in environmental science*, 6.
- BANERJEE, D. & GANGULY, S. 2023. A Review on the Research Advances in Groundwater– Surface Water Interaction with an Overview of the Phenomenon. *Water (Basel),* 15, 1552.
- BARNETT, B., LR, T., V, P., RE, E., RJ, H., L, P., S, R., AD, W., A, K. & A, B. 2012. Australian groundwater modelling guidelines, Waterlines report. *In:* NATIONAL WATER COMMISSION (ed.). Canberra.
- BARNETT, S. R. 2009. Groundwater resource assessment of the Baroota Prescribed Water Resources Area. *In:* DEPARTMENT OF WATER, L. A. B. C. (ed.). South Australia. .
- BATELAAN, O. & DE SMEDT, F. 2007. GIS-based recharge estimation by coupling surface—subsurface water balances. *Journal of hydrology (Amsterdam)*, 337, 337-355.
- BATLLE-AGUILAR, J. & COOK, P. G. 2012. Transient infiltration from ephemeral streams: A field experiment at the reach scale. *Water resources research*, 48, n/a.
- BIRON, P. M., CHONÉ, G., BUFFIN-BÉLANGER, T., DEMERS, S. & OLSEN, T. 2013. Improvement of streams hydro-geomorphological assessment using LiDAR DEMs. *Earth surface processes and landforms*, 38, 1808-1821.
- BLASCH, K., FERRÉ, T. P. A., HOFFMANN, J., POOL, D., BAILEY, M., CORDOVA, J., SCANLON, B. R., PHILLIPS, F. M. & HOGAN, J. F. 2004. Processes Controlling Recharge Beneath Ephemeral Streams in Southern Arizona. Washington, D. C: American Geophysical Union.
- BOAS, T. & MALLANTS, D. 2022. Episodic extreme rainfall events drive groundwater recharge in arid zone environments of central Australia. *Journal of Hydrology: Regional Studies*, 40, 101005.
- BOM Climate Data Online. Bureau of Meteorology.
- BOULTON, A. J., FINDLAY, S., MARMONIER, P., STANLEY, E. H. & VALETT, H. M. 1998. THE FUNCTIONAL SIGNIFICANCE OF THE HYPORHEIC ZONE IN STREAMS AND RIVERS. *Annual Review of Ecology, Evolution, and Systematics*, 29, 59-81.
- BRUNNER, G. W. 2010. *HEC-RAS, River Analysis System User's Manual, version 4.1*, U.S. Army Corps of Eng., Hydrol. Eng. Cent., Davis, Calif.
- BRUNNER, P., COOK, P. G. & SIMMONS, C. T. 2009. Hydrogeologic controls on disconnection between surface water and groundwater. *Water resources research*, 45, n/a.
- BRUNNER, P., COOK, P. G. & SIMMONS, C. T. 2010. Disconnected Surface Water and Groundwater: From Theory to Practice. *Groundwater*, 49, 460-467.
- BRUNNER, P., COOK, P. G. & SIMMONS, C. T. 2011. Disconnected Surface Water and Groundwater: From Theory to Practice. *Ground water,* 49, 460-467.
- CAMPOREALE, C., PERUCCA, E., RIDOLFI, L. & GURNELL, A. M. 2013. MODELING THE INTERACTIONS BETWEEN RIVER MORPHODYNAMICS AND RIPARIAN VEGETATION. *Reviews of Geophysics*, 51, 379-414.
- CHOW, V. T. 1959. Open Channel Hydraulics, McGraw-Hill, New York.

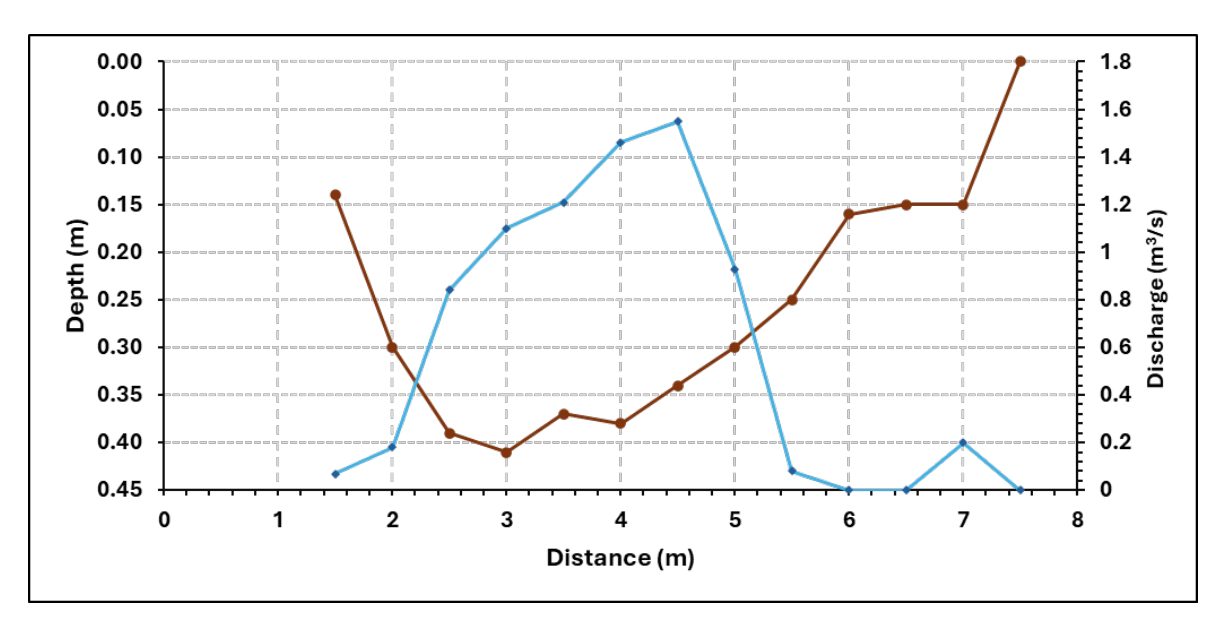
- COOK, P. G., BRUNNER, P., SIMMONS, C. T. & LAMONTAGNE, S. 2010. What is a Disconnected Stream? . *Groundwater 2010, The Challenge of sustainable management*. National Convection Centre, Canberra.
- CUTHBERT, M. O., ACWORTH, R. I., ANDERSEN, M. S., LARSEN, J. R., MCCALLUM, A. M., RAU, G. C. & TELLAM, J. H. 2016. Understanding and quantifying focused, indirect groundwater recharge from ephemeral streams using water table fluctuations. *Water resources research*, 52, 827-840.
- DEW 2021. Baroota Prescribed Water Resources Area groundwater resources assessment. *In:* WATER, D. F. E. A. (ed.). Adelaide: Government of South Australia.
- DEW November 2020. Baroota Prescribed Water Resources Area groundwater resource assessment. *In:* DEPARTMENT FOR ENVIRONMENT AND WATER (ed.). Adelaide: Government of South Australia.
- DEWNR 2014. Baroota PWRA Surface Water Status Report 2010-11. *In:* GOVERNMENT OF SOUTH AUSTRALIA, T. D. O. & ENVIRONMENT, W. A. N. R. (eds.). Adelaide.
- DOGRAMACI, S., FIRMANI, G., HEDLEY, P., SKRZYPEK, G. & GRIERSON, P. F. 2015. Evaluating recharge to an ephemeral dryland stream using a hydraulic model and water, chloride and isotope mass balance. *Journal of hydrology (Amsterdam)*, 521, 520-532.
- DOMENICO, P. A., SCHWARTZ, F. W. & ZHANG, H. 1998. *Physical and chemical hydrogeology,* New York, Wiley.
- EVANS, S. 2004a. Baroota Groundwater Resource-Monitoring Review and Augmentation. *In:* WATER, D. O. & CONSERVATION, L. A. B. (eds.). Adelaide, SA.
- EVANS, S. 2004b. Baroota Groundwater Resource-Monitoring Review and Augmentation. *In:*DEPARTMENT OF WATER, L. A. B. C. (ed.). Adelaide, SA: Department of Water, Land and Biodiversity Conservation.
- FETTER, C. W. 2001. Applied hydrogeology, Upper Saddle River, N. J, Pearson Education.
- GHOSH, B. & PEKKAT, S. 2019. An Appraisal on the Interpolation Methods Used for Predicting Spatial Variability of Field Hydraulic Conductivity. *Water Resources Management*, 33, 2175-2190.
- GUTIERREZ-JURADO, K. Y., PARTINGTON, D. & SHANAFIELD, M. 2021. Taking theory to the field: streamflow generation mechanisms in an intermittent Mediterranean catchment. Hydrology and earth system sciences, 25, 4299-4317.
- HATCH, C. E., FISHER, A. T., RUEHL, C. R. & STEMLER, G. 2010. Spatial and temporal variations in streambed hydraulic conductivity quantified with time-series thermal methods. *Journal of hydrology (Amsterdam)*, 389, 276-288.
- HIPÓLITO, J. N. & LOUREIRO, J. M. 1988. Analysis of some velocity-area methods for calculating open channel flow. *Hydrological sciences journal*, 33, 311-320.
- HUNT, R. J. & FEINSTEIN, D. T. 2012. MODFLOW-NWT: Robust Handling of Dry Cells Using a Newton Formulation of MODFLOW-2005. *Ground water*, 50, 659-663.
- IRVINE, D. J., BRUNNER, P., FRANSSEN, H.-J. H. & SIMMONS, C. T. 2012. Heterogeneous or homogeneous? Implications of simplifying heterogeneous streambeds in models of losing streams. *Journal of hydrology (Amsterdam)*, 424-425, 16-23.
- KOCH, H., SILVA, A. L. C., LIERSCH, S., DE AZEVEDO, J. R. G. & HATTERMANN, F. F. 2020. Effects of model calibration on hydrological and water resources management simulations under climate change in a semi-arid watershed. *Climatic change*, 163, 1247-1266.
- LAMONTAGNE, S., LEANEY, F. W. & HERCZEG, A. L. 2005. Groundwater-surface water interactions in a large semi-arid floodplain: implications for salinity management. *Hydrological Processes*, 19, 3063-3080.
- LEVICK, L., FONSECA, J., GOODRICHO, D., HERNANDEZ, M., SEMMENS, D., STROMBERG, J., R. LEIDY, M., SCIANNI, GUERTIN, D. P., TLUCZEK, M. & KEPNER, W. 2008. The Ecological and Hydrological Significance of Ephemeral and Intermittent Streams in the Arid and Semi-arid American

- Southwest.: U.S. Environmental Protection Agency and USDA/ARS Southwest Watershed Research Center.
- LU, C., LU, W., SUN, Q., HE, X., YAN, L., QIN, T., WU, C., HAN, S., WU, Z. & WU, W. 2024. Simulation of Drying-Rewetting Processes in Numerical Groundwater Models Using a New Picard Iteration-Based Method. *Water resources research*, 60, n/a.
- MAXWELL, R. M. & KOLLET, S. J. 2008. Interdependence of groundwater dynamics and landenergy feedbacks under climate change. *Nature Geoscience*, **1**, 665-669.
- MIN, L., VASILEVSKIY, P. Y., WANG, P., POZDNIAKOV, S. P. & YU, J. 2020. Numerical Approaches for Estimating Daily River Leakage from Arid Ephemeral Streams. *Water*, 12, 499.
- MOLNAR, P., DENSMORE, A. L., MCARDELL, B. W., TUROWSKI, J. M. & BURLANDO, P. 2010. Analysis of changes in the step-pool morphology and channel profile of a steep mountain stream following a large flood. *Geomorphology*, 124, 85-94.
- MORIN, E., GRODEK, T., DAHAN, O., BENITO, G., KULLS, C., JACOBY, Y., LANGENHOVE, G. V., SEELY, M. & ENZEL, Y. 2009. Flood routing and alluvial aquifer recharge along the ephemeral arid Kuiseb River, Namibia. *Journal of hydrology (Amsterdam)*, 368, 262-275.
- NAGANNA, S. R., DEKA, P. C., CH, S. & HANSEN, W. F. 2017. Factors influencing streambed hydraulic conductivity and their implications on stream-aquifer interaction: a conceptual review. *Environmental Science and Pollution Research*, 24, 24765-24789.
- NISWONGER, R. G., PANDAY, S. & IBARAKI, M. 2011. MODFLOW-NWT, A Newton formulation for MODFLOW-2005: U.S. Geological Survey Techniques and Methods 6–A37.
- NISWONGER, R. G., PRUDIC, D. E., POHLL, G. & CONSTANTZ, J. 2005. Incorporating seepage losses into the unsteady streamflow equations for simulating intermittent flow along mountain front streams. *Water resources research*, 41, n/a.
- NOORDUIJN, S. L., SHANAFIELD, M., TRIGG, M. A., HARRINGTON, G. A., COOK, P. G. & PEETERS, L. 2014. Estimating seepage flux from ephemeral stream channels using surface water and groundwater level data. *Water resources research*, 50, 1474-1489.
- QUICHIMBO, E. A., SINGER, M. B. & CUTHBERT, M. O. 2020. Characterising groundwater–surface water interactions in idealised ephemeral stream systems. *Hydrological processes*, 34, 3792-3806.
- RABANAQUE, M. P., MARTÍNEZ-FERNÁNDEZ, V., CALLE, M. & BENITO, G. 2022. Basin-wide hydromorphological analysis of ephemeral streams using machine learning algorithms. *Earth Surface Processes and Landforms*, 47, 328-344.
- SA ARID LANDS LANDSCAPE BOARD June 2010. River Red Gum Woodlands of watercourses and floodplains. *In:* BOARD, S. A. A. L. N. R. M. (ed.). South Australia.
- SHANAFIELD, M. & COOK, P. G. 2014. Transmission losses, infiltration and groundwater recharge through ephemeral and intermittent streambeds: A review of applied methods. *Journal of hydrology (Amsterdam)*, 511, 518-529.
- SHANAFIELD, M., COOK, P. G., BRUNNER, P., MCCALLUM, J. & SIMMONS, C. T. 2012. Aquifer response to surface water transience in disconnected streams. *Water resources research*, 48, n/a.
- SHANAFIELD, M., NISWONGER, R. G., PRUDIC, D. E., POHLL, G., SUSFALK, R. & PANDAY, S. 2014. A method for estimating spatially variable seepage and hydraulic conductivity in channels with very mild slopes. *Hydrological processes*, 28, 51-61.
- SOPHOCLEOUS, M. 2002. Interactions between groundwater and surface water: the state of the science. *Hydrogeology Journal*, 10, 52-67.
- THE LANDSCAPE BOARDS SOUTH AUSTRALIA. 2025a. *Baroota and Beetaloo water releases* [Online]. Available: <a href="https://www.landscape.sa.gov.au/ny/projects/environmental-and-cultural-flows/environmental-water-releases">https://www.landscape.sa.gov.au/ny/projects/environmental-and-cultural-flows/environmental-water-releases</a> [Accessed].
- THE LANDSCAPE BOARDS SOUTH AUSTRALIA. 2025b. *Baroota Water Allocation Plan* [Online]. The Landscape Boards South Australia. Available:

- https://www.landscape.sa.gov.au/ny/water/water-allocation-plans/baroota-wap [Accessed].
- VILLENEUVE, S., COOK, P. G., SHANAFIELD, M., WOOD, C. & WHITE, N. 2015. Groundwater recharge via infiltration through an ephemeral riverbed, central Australia. *Journal of arid environments*, 117, 47-58.
- WANG, P., POZDNIAKOV, S. P. & VASILEVSKIY, P. Y. 2017. Estimating groundwater-ephemeral stream exchange in hyper-arid environments: Field experiments and numerical simulations. *Journal of hydrology (Amsterdam)*, 555, 68-79.
- WARIX, S. R., NAVARRE-SITCHLER, A., MANNING, A. H. & SINGHA, K. 2023. Local Topography and Streambed Hydraulic Conductivity Influence Riparian Groundwater Age and Groundwater-Surface Water Connection. *Water resources research*, 59.
- WATER, D. F. 2009-10. Baroota PWRA Groundwater Status Report.
- WINTER, T. C., HARVEY, J. W., FRANKE, O. L. & ALLEY, W. M. 1998. Ground water and surface water: a single resource. *In:* SURVEY, U. S. G. (ed.).
- WOHL, E., ANGERMEIER, P. L., BLEDSOE, B., KONDOLF, G. M., MACDONNELL, L., MERRITT, D. M., PALMER, M. A., POFF, N. L. & TARBOTON, D. 2005. River restoration. *Water Resources Research*, 41.
- ZHONG, Y., ZHOU, A., DU, J., TENG, J. & SHEN, S.-L. 2023. Modified Kozeny-Carman equation for estimating hydraulic conductivity in nanoscale pores of clayey soils with active surfaces. *Journal of Hydrology*, 626, 130209.

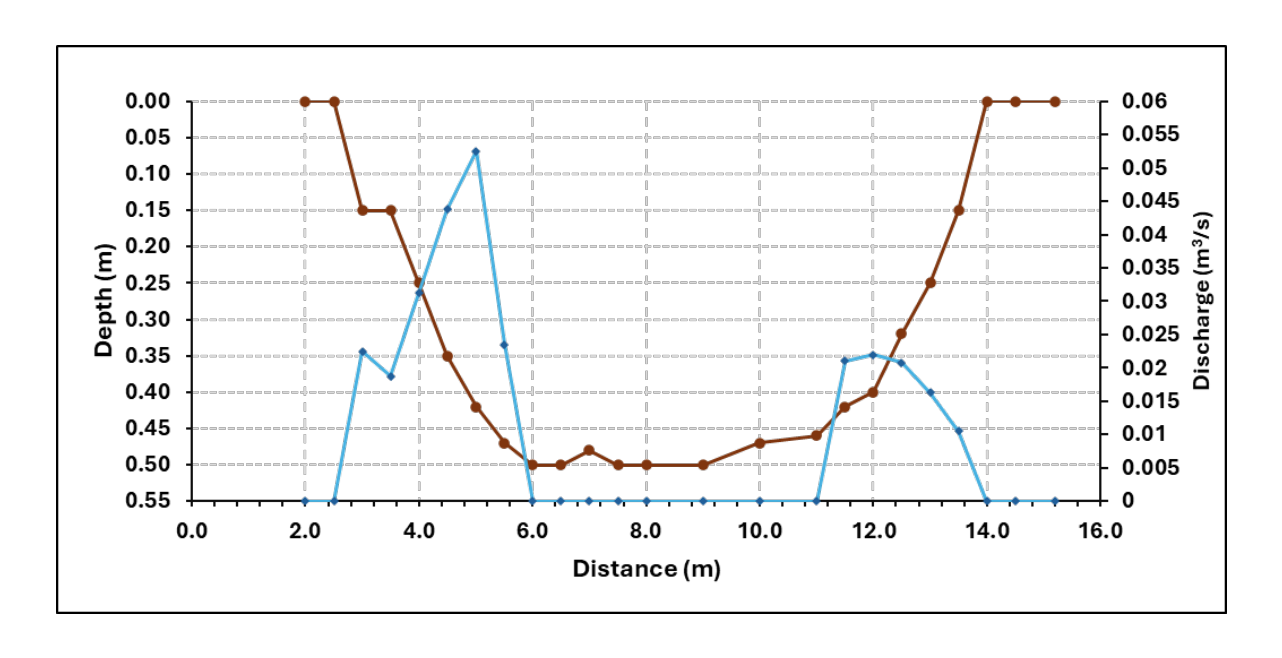
# 8 Appendices

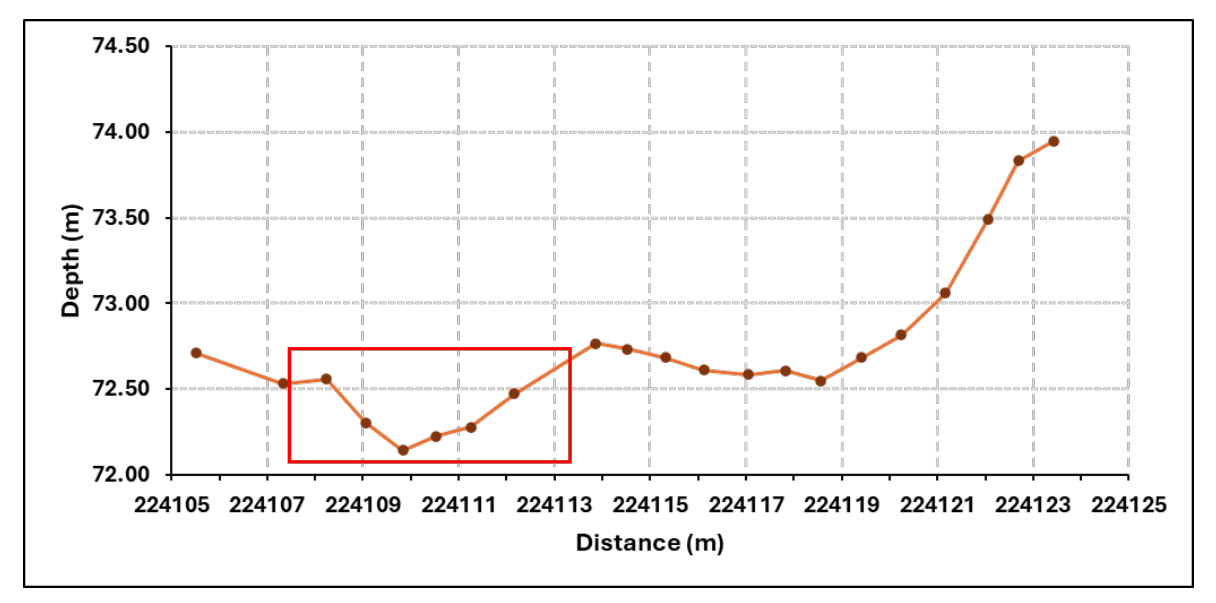
# 8.1 Creek Geometry and Gauging measurement



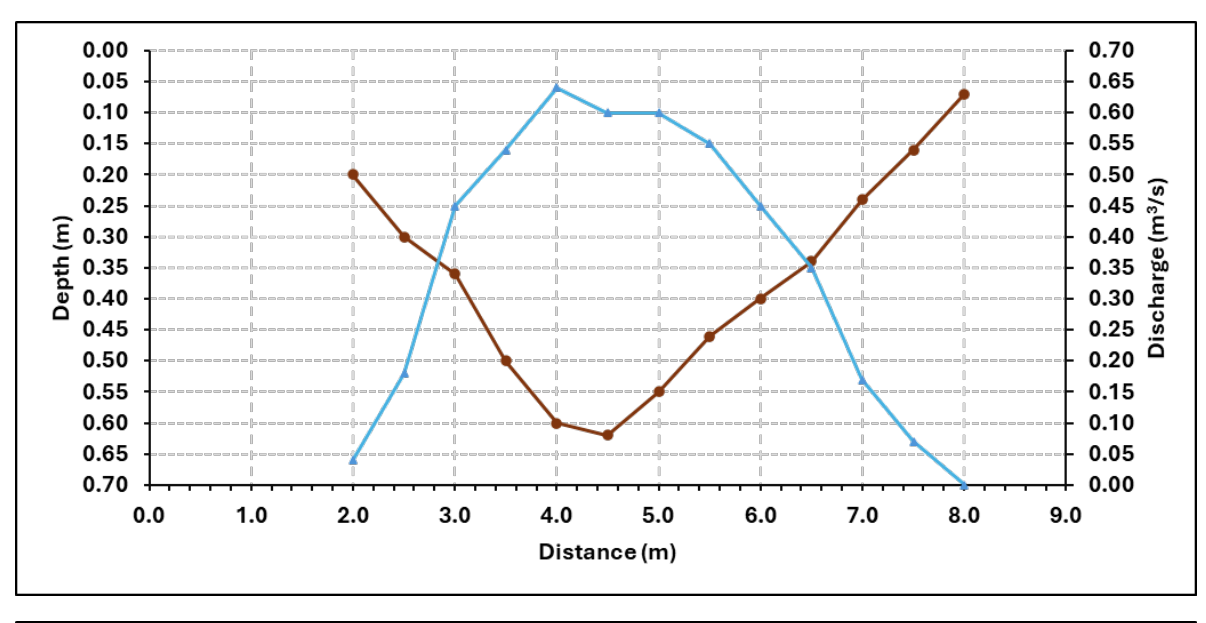


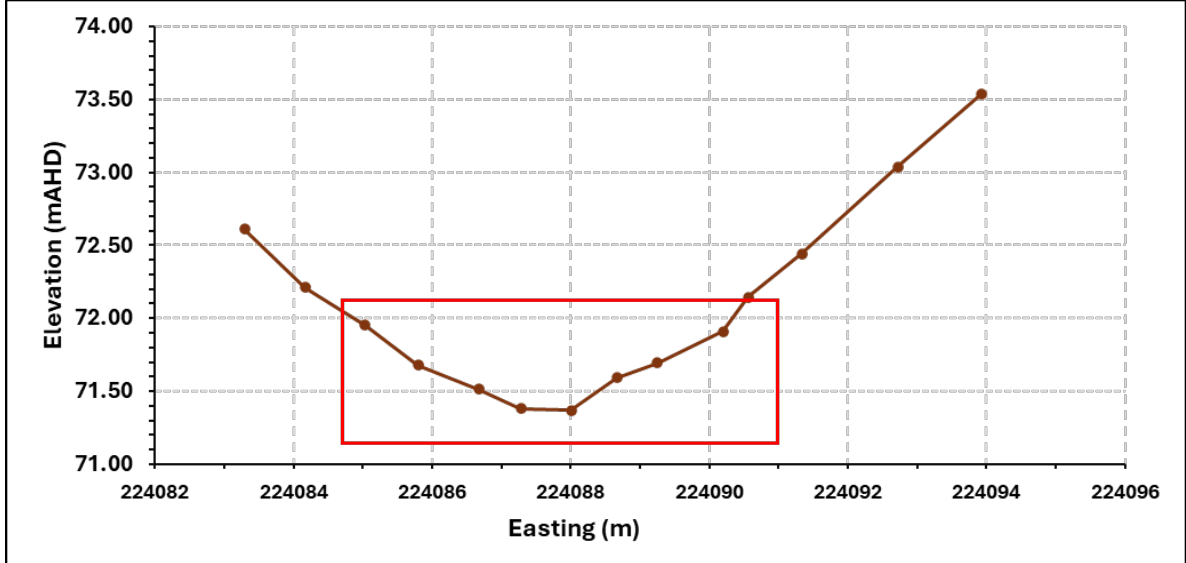
**Supplementary Figure 1** Creek geometry at SW-5 in Baroota Creek, illustrating data collection methods. Top: Cross-section generated from manual gauging measurements. Bottom: Cross-section captured using GNSS data collection, showing differing levels of detail or coverage. The area corresponding to the gauging measurement is highlighted by a red box in the GNSS cross-section.



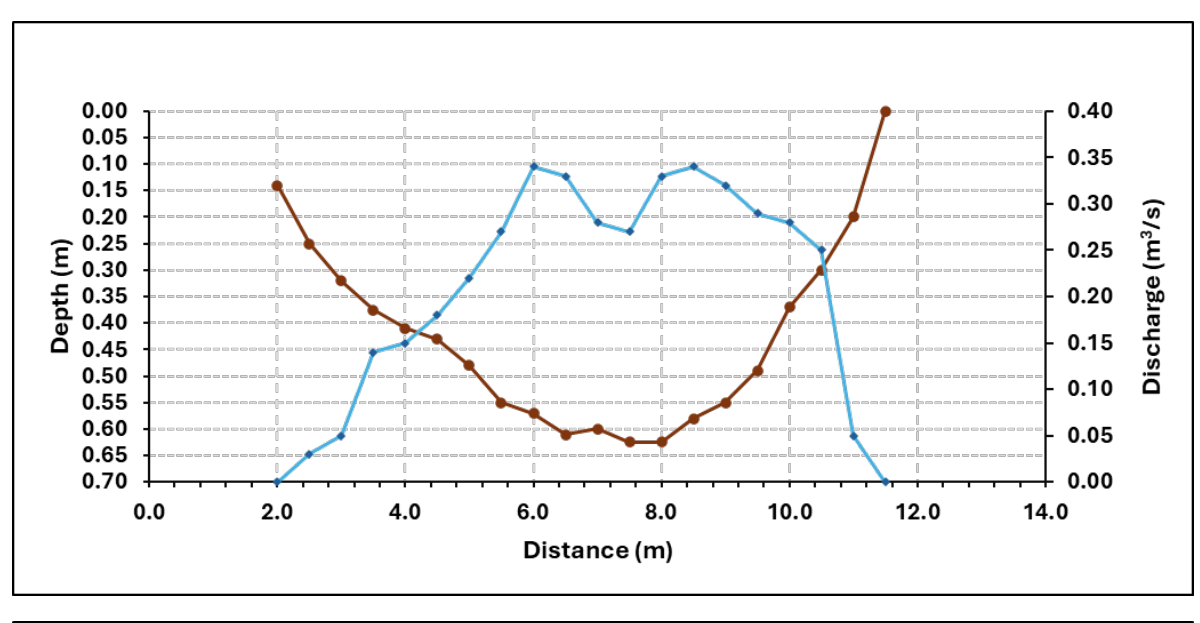


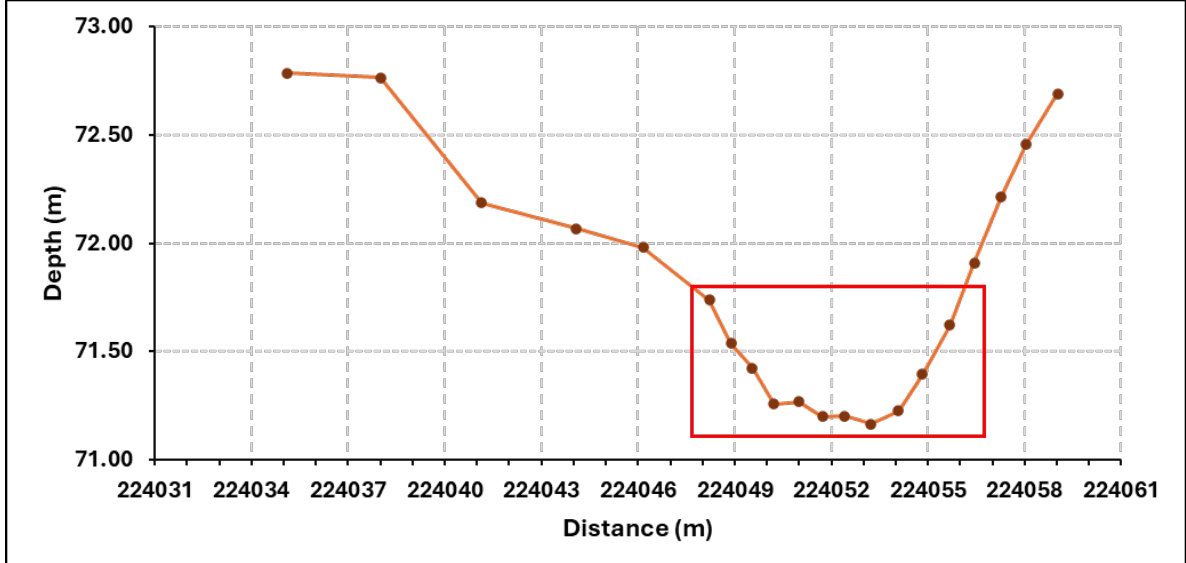
**Supplementary Figure 2** Creek geometry at SW-4 in Baroota Creek, illustrating data collection methods. Top: Cross-section generated from manual gauging measurements. Bottom: Cross-section captured using GNSS data collection, showing differing levels of detail or coverage. The area corresponding to the gauging measurement is highlighted by a red box in the GNSS cross-section.



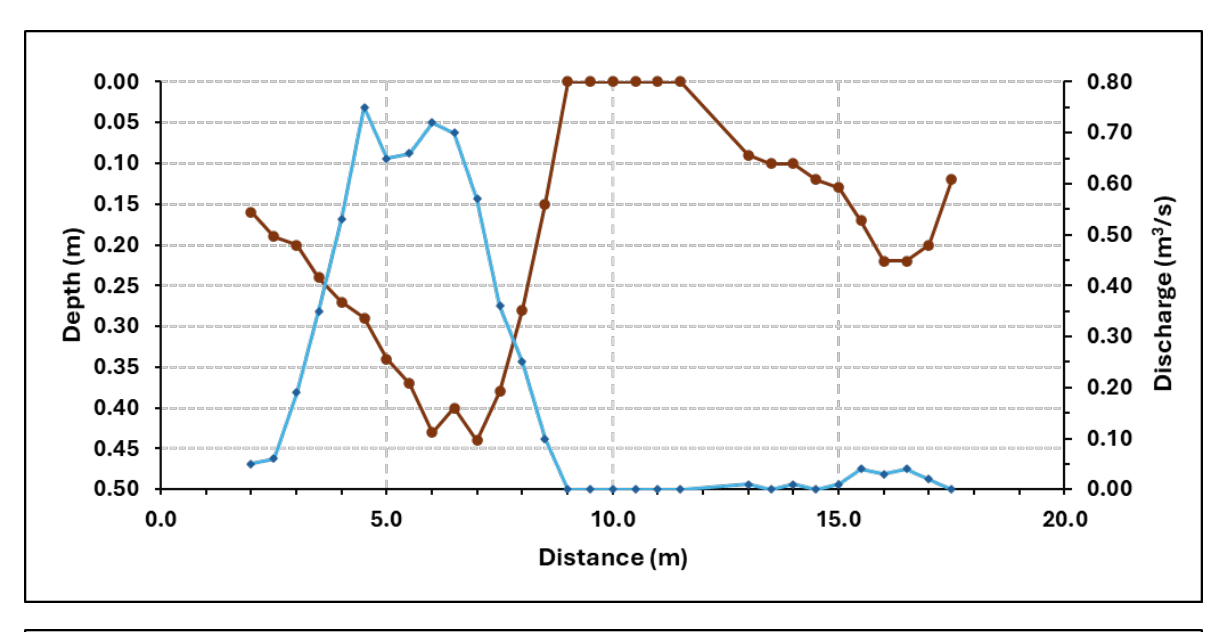


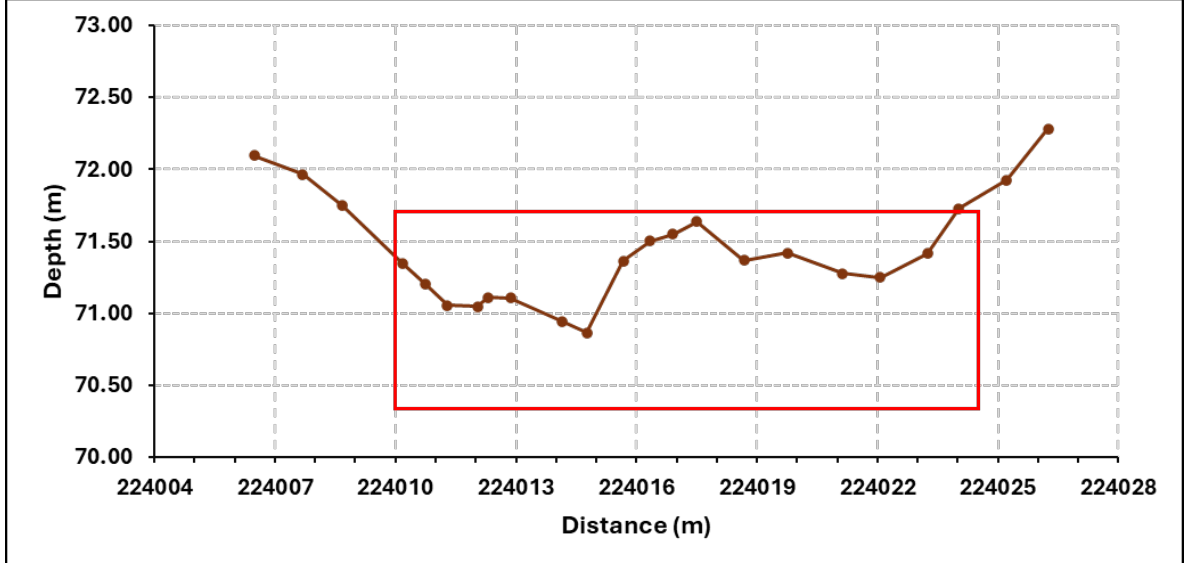
**Supplementary Figure 3** Creek geometry at SW-3 in Baroota Creek, illustrating data collection methods. Top: Cross-section generated from manual gauging measurements. Bottom: Cross-section captured using GNSS data collection, showing differing levels of detail or coverage. The area corresponding to the gauging measurement is highlighted by a red box in the GNSS cross-section.



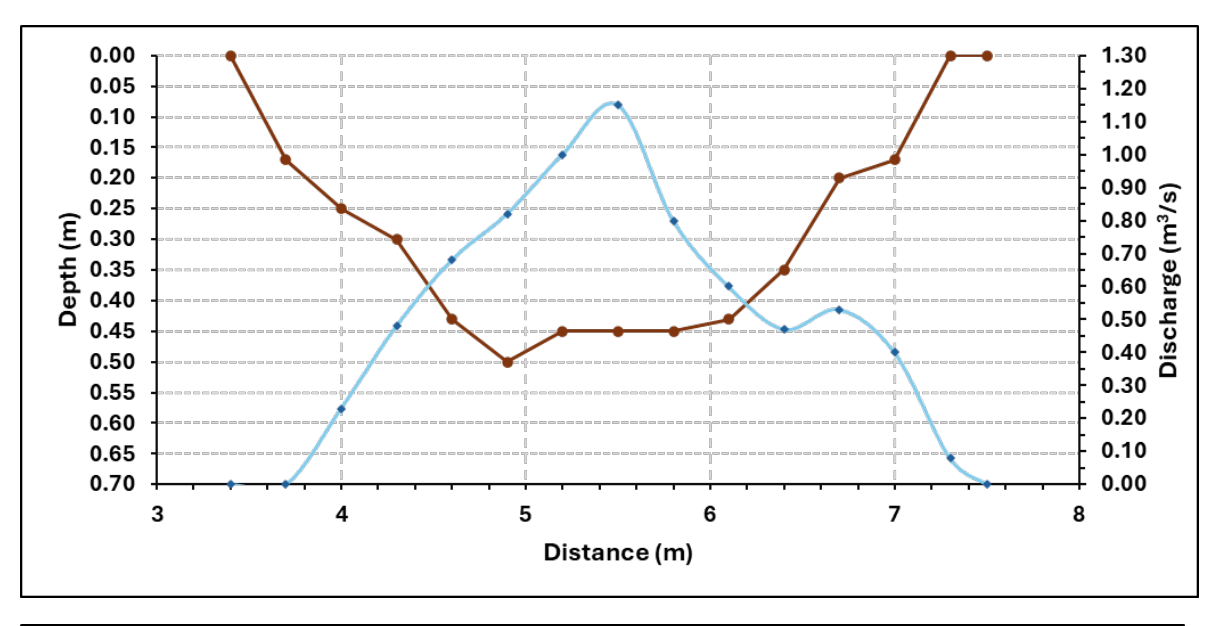


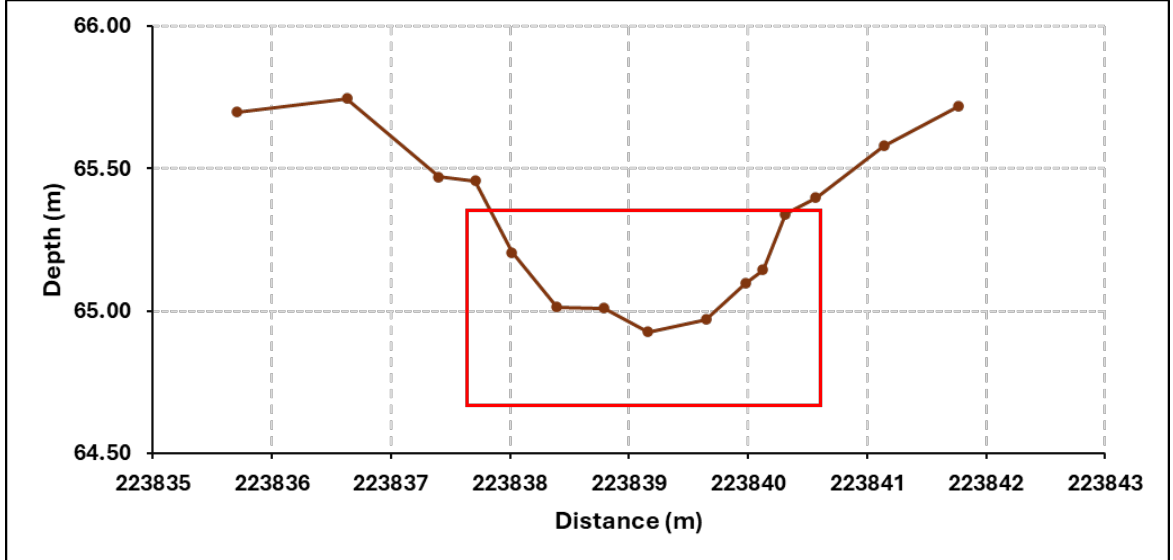
**Supplementary Figure 4** Creek geometry at SW-2 in Baroota Creek, illustrating data collection methods. Top: Cross-section generated from manual gauging measurements. Bottom: Cross-section captured using GNSS data collection, showing differing levels of detail or coverage. The area corresponding to the gauging measurement is highlighted by a red box in the GNSS cross-section.



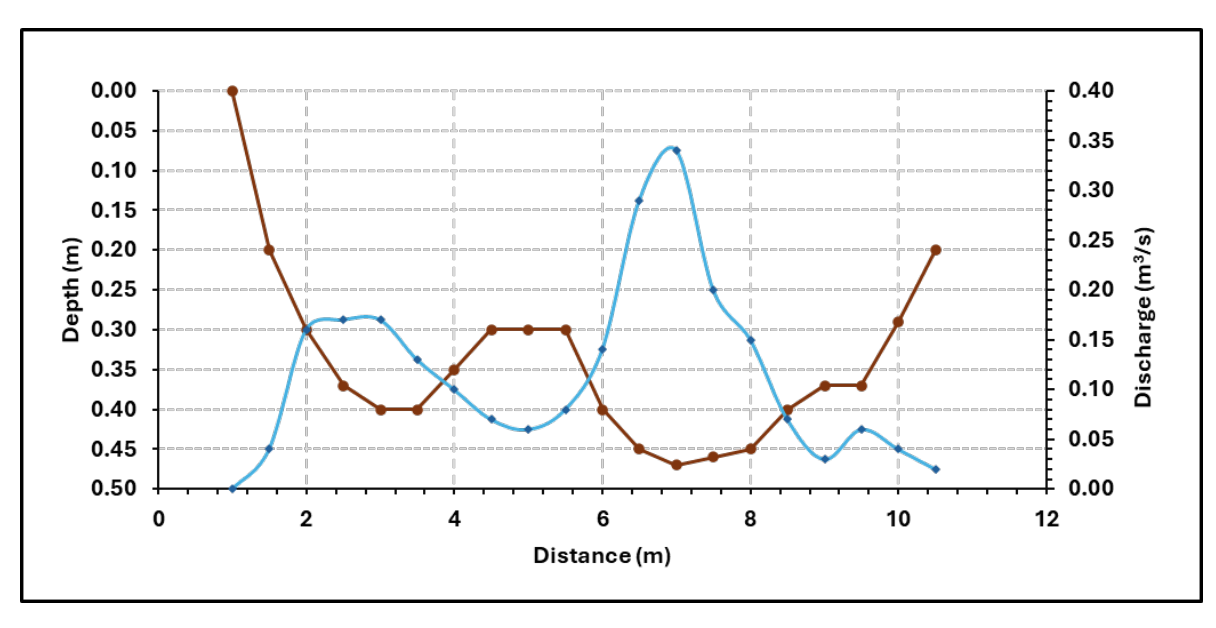


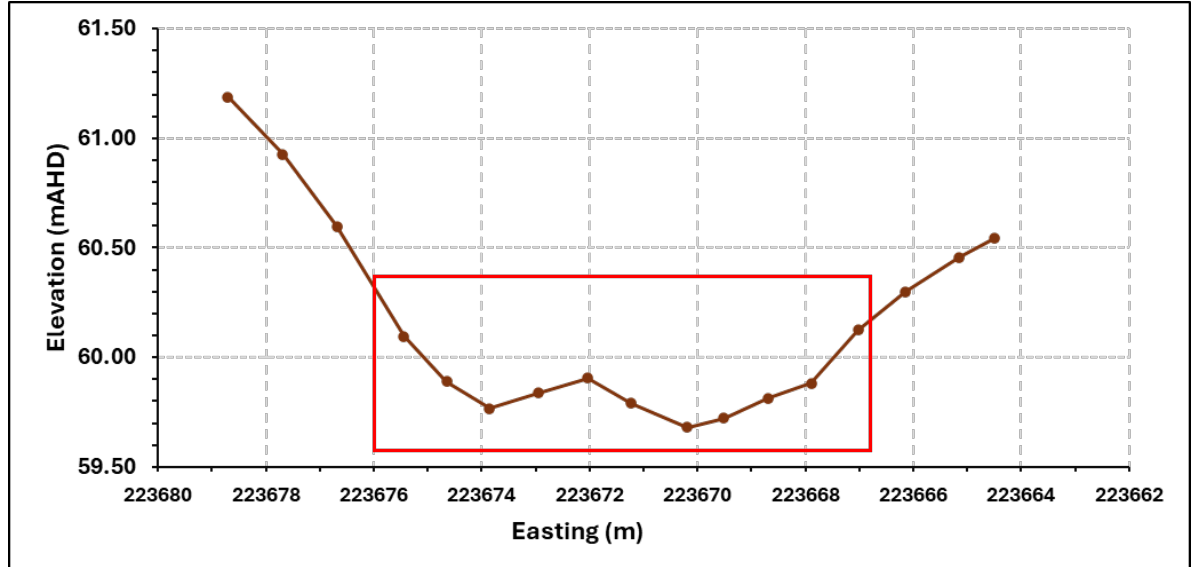
**Supplementary Figure 5** Creek geometry at SW-1 in Baroota Creek, illustrating data collection methods. Top: Cross-section generated from manual gauging measurements. Bottom: Cross-section captured using GNSS data collection, showing differing levels of detail or coverage. The area corresponding to the gauging measurement is highlighted by a red box in the GNSS cross-section.





**Supplementary Figure 6** Creek geometry at SW-6 in Baroota Creek, illustrating data collection methods. Top: Cross-section generated from manual gauging measurements. Bottom: Cross-section captured using GNSS data collection, showing differing levels of detail or coverage. The area corresponding to the gauging measurement is highlighted by a red box in the GNSS cross-section.





**Supplementary Figure 7** Creek geometry at SW-7 in Baroota Creek, illustrating data collection methods. Top: Cross-section generated from manual gauging measurements. Bottom: Cross-section captured using GNSS data collection, showing differing levels of detail or coverage. The area corresponding to the gauging measurement is highlighted by a red box in the GNSS cross-section.

# 8.2 Simulation period

**Supplementary Table 1** Simulation period of numerical modelling in different stress periods in Baroota Creek between August 22-30 2024.

Stress Period	Day	Time	Flood Frontwave observation	Time length (seconds)	Accumulated time (seconds)	Model state
1	22/08/24	16.59	1	0	0	Steady
2	22/08/25	19.53	2	10440	10440	Transient
3	23/08/23	11.28	3	56100	66540	Transient
4	23/08/24	16.59		19860	86400	Transient
5	24/08/24	16.59		86400	172800	Transient
6	24/08/25	21.30	4	16260	189060	Transient
7	25/08/23	11.54	5	49380	238440	Transient
8	25/08/24	16.59		20760	259200	Transient
9	26/08/23	4.59		43200	302400	Transient
10	26/08/24	16.59		43200	345600	Transient
11	27/08/23	4.59		43200	388800	Transient
12	27/08/24	16.59		43200	432000	Transient
13	28/08/23	4.59		43200	475200	Transient
14	28/08/24	16.59		43200	518400	Transient
15	29/08/23	4.59		43200	561600	Transient
16	29/08/24	16.59		43200	604800	Transient
17	30/08/23	4.59		43200	648000	Transient
18	30/08/24	12.00	6	25260	673260	Transient